Modelling primary production: multitude of theories, or multitude of languages?

Jozef Skákala[1,2], Shubha Sathyendranath[1,2], Yuri Artioli[1], Deep S Banerjee[1,2], Heather Bouman[3], Robert J.W. Brewin[4], Momme Butenschön[5], Stefano Ciavatta[6], Stephanie Dutkiewicz[7], Yanna Fidai[1], David Ford[8], Grinson George[9], Karen Guihou[6], Bror Jönsson[10], Marija Bačeković Koloper[11], Žarko Kovač[11], Lekshmi Krishnakumary[1], Gemma Kulk[1,2], Charlotte Laufkötter[12], Gennadi Lessin[1], Jann Paul Mattern[13], Angélique Melet[6], Alexandre Mignot[6], David Moffat[1,2], Fanny Monteiro[14], Mayra Rodriguez Bennadji[3], Cécile Rousseaux[15], Ranjini Swaminathan[16], Osvaldo Ulloa[17] and Jerry Tjiputra[18]

[1]Plymouth Marine Laboratory, UK,
[2]National Centre for Earth Observation, UK,
[3]University of Oxford, UK,
[4]University of Exeter, UK,
[5]Euro-Mediterranean Center on Climate Change (CMCC), Italy,
[6]Mercator Ocean International, France,
[7]Massachusetts Institute of Technology, USA,
[8]Met Office, UK,
[9]Central Marine Fisheries Research Institute, India,
[10]University of New Hampshire, USA,
[11]University of Split, Croatia,
[12]University of Bern, Switzerland,
[13]University of California, Santa Cruz, USA,
[14]University of Bristol, UK,
[15]National Aeronautics and Space Administration (NASA), USA,
[16]University of Reading, UK,
[17]University de Concepcion, Chile,
[18]NORCE Research AS, Norway

Correspondence to: Jozef Skakala (jos@pml.ac.uk)

Abstract. Marine primary production, converting approximately 50GtC per year, is an important component of the global carbon cycle, and a major determinant of past, present and future climate. Large-scale, long-term estimates of marine primary production rely primarily on two types of models: satellite-based models that make extensive use of remote-sensing data, and ecosystem models providing numerical simulation of ecological processes embedded in general ocean circulation models. Intercomparison exercises of model outputs (both within and across the two model types) have consistently revealed high discrepancies between estimated global ocean primary production, including divergent magnitudes and even opposite trends. Comparisons of model results with in-situ observations have also revealed large uncertainties in marine primary production estimates. These uncertainties limit the applications of these models, especially in the climate context, where an important question is whether climate change will drive significant future changes in regional or global primary production. Both satellite-based and ecosystem model equations rely on a range of fixed parameters, whose values need to be carefully estimated and tested. In this paper, we suggest that such model parameters represent an underappreciated but important source of inter-model differences. With the proliferation of both satellite and in situ observations of relevant variables at global scales and the availability of powerful statistical tools in data assimilation and machine

47   learning, we argue that time is right to systematically examine model parameters and gain insights into how they

48   may vary spatially and temporally. We emphasize that such spatio-temporal variability can be easily theoretically

49   justified for the models with complexity similar to the satellite models, or the ecosystem models commonly used

50   within Earth System Models (ESMs) in climate studies. We argue that the spatially and temporally varying

51   parameter values provide a strong reason to anticipate unification of models, which would otherwise appear

52   structurally different. A better understanding of model parameter roles could therefore reduce discrepancies

53   among the primary production models and improve the reliability of marine primary production projections.

54

55

56   **1.   Introduction**

57   The climate problem is highly complex, the stakes are very high, and substantial knowledge gaps remain,

58   especially in the ocean biogeochemistry domain (Kwiatkowski *et al.,* 2020). More broadly, the need to address

59   complex issues related to the carbon cycle, ecosystem services and biogeochemistry through Earth System Models

60   (ESMs), e.g. in the context of climate adaptation and resilience, has been highlighted by expert groups in Hewitt

61   *et al.* (2021). Similarly, Jones *et al.* (2024) focus on modelling priorities to support international climate policy.

62   In their assessment, they emphasise the value of "a coordinated, internally consistent set of simulations, data, and

63   knowledge to support Intergovernmental Panel on Climate Change (IPCC) assessments" and outline multiple

64   applications of Coupled Model Intercomparison Project (CMIP) projections. These include investigations of

65   threats to marine ecosystems (which have consequences for the ocean's ability to buffer climate change, Tjiputra

66   *et al.,* 2025) and downstream services under various climate scenarios and associated risks of tipping points. Jones

67   *et al.* (2024) also state that improving confidence in future projections requires models to reproduce the observed

68   historical period. Furthermore, they identify parameter uncertainty as one of the key elements of uncertainty in

69   climate models. The European Commission (2024) emphasised the need for improved projections of future

70   possible impacts to understand better the relation between physiological processes and environmental variables.

71   Against this background and in line with the recommendations of expert bodies, this review focuses on the

72   climate priority challenge associated with marine ecosystem and biogeochemistry modelling, with a particular

73   focus on marine primary production. Phytoplankton primary production (PP), the process by which marine

74   autotrophs convert CO_2 into organic matter through photosynthesis, is a major component of the ocean and

75   planetary carbon cycle. Currently estimated at around 50 Pg C y^{-1} (Kulk *et al.* 2020, 2021), the magnitude of

76   marine PP is five times the estimated fossil fuel emissions of 10 Pg C y^{-1} in 2022 and nearly 20 times the net ocean

77   carbon sink (Friedlingstein *et al.* 2024). Its magnitude is comparable to that of terrestrial primary production

78   (Lurin *et al.* 1994; Longhurst *et al.* 1995; Field *et al.* 1998; Friedlingstein *et al.* 2024). A key question in climate

79   research is whether the current levels of marine PP can be maintained under climate change (Tagliabue *et al.,*

80   2021), at a time when marine ecosystems are increasingly threatened by a variety of sources, including ocean

81   acidification (Jin *et al.,* 2020, Dai *et al.,* 2025), rising seawater temperatures (Kwiatkowski *et al.,* 2020),

82   intensified storminess over the oceans (Gastineau and Soden, 2009, Young *et al.,* 2019, Gentille *et al.,* 2023, Liu

83   *et al.,* 2024), ocean deoxygenation (Schmidtko *et al.,* 2017), modified current and stratification influencing surface

84   nutrients (Maishal, 2024), as well as changes in aerial nutrient supply (Bergas-Masso *et.al.,* 2025), biodiversity

85   loss (Luypaert *et al*., 2020), and sea-ice loss (Myksvoll *et al.,* 2023). In this review we consider PP estimated

86   from two types of models: "satellite-based models" that utilize remote-sensing data together with statistical

87   algorithms, whose parameters are informed by in situ measurements, to calculate PP, and mechanistic ecosystem

88   models which use numerical methods to solve a set of differential equations representing ecological processes,

89   with one output being PP.

90   When discussing marine primary PP, it is important to keep track of its different components. Theoretically,

91   PP before any of the loss terms are considered is referred to as gross PP (GPP); once the respiration by marine

92   autotrophs is subtracted from GPP we obtain net PP (NPP). GPP can also be partitioned according to whether

93   only the organic carbon fixed into particulate material is considered (production of particulate organic carbon), or

94   if the exudates (dissolved organic matter) are also included in the estimate (production of total organic carbon,

95   Regaudie-de-Gioux *et al.* 2014). While ecosystem models can make explicit distinction between these

96   components, it is not always straightforward to measure each of the components, often due to lack of experimental

97   methodologies that would differentiate clearly between them (IOCCG, 2022). In this review, we focus mainly on

98   GPP as computed in ecosystem models. For satellite-based estimates, we treat primary production derived from

99   in-situ experiments measuring short (1-4 hours) incubations as GPP, and those derived from experiments

100   measuring longer (12-24 hour) incubations as NPP, while fully recognising that the distinction is not that clear

101   cut (e.g., Halsey *et al.* 2011). It should be noted that estimates of the magnitude of losses due to respiration vary

102   considerably. Some estimates place it at about 30% of gross primary production (e.g., Platt *et al.* 1991), while

103   some other estimates are higher (e.g., 60% according to Halsey *et al.* 2011). Platt and Sathyendranath (1988)

104   compared daily water-column primary production computed on the basis of short incubations with those measured

105   in situ over daily time scales, and showed the two sets of independent estimates to be comparable, which points

106   to low respiration losses. Also, satellite-based estimates of NPP (Behrenfeld and Falkowski 1997) tend to be

107   roughly the same or higher than GPP (Longhurst *et al.* 1995). Since, by definition, NPP cannot be greater than

108   GPP, these comparisons reveal a great deal of uncertainty in respiration, or in PP computed using different

109   approaches, when compared with each other.

110

111

2.   Background

113   Considerable differences exist in model-based estimates (here and elsewhere, we use "models'' without a

114   qualifier, to mean both satellite-based and ecosystem models) of the current and past global PP in the ocean, and

115   in ecosystem-model based projections into the future.

116   Satellite-based estimates of global marine PP are converging around 45-55 Pg C y^{-1} (Figure 1A). These

117   estimates were obtained from both multi-sensor products of the Ocean Colour Climate Change Initiative (OC-

118   CCI; version 6, Sathyendranath *et al.* 2019, Kulk *et al.* 2020, 2021), as well as from single-sensor products of the

119   Oregon State University (http://orca.science.oregonstate.edu/), which include the Carbon, Absorption, and

120   Fluorescence Euphotic-resolving (CAFE) model (Silsbe *et al.* 2016; 2025), Carbon-Based Primary Productivity

121   Model (CBPM; Westberry *et al.* 2008), the Vertically Generalised Production Model (VGPM; Behrenfeld and

122   Falkowski 1997) and the VGPM-Eppley model (which incorporates the Eppley (1972) temperature function).

123   However, we note that much higher values (up to 67 Pg C y^{-1}) and lower values ($\leq$45 Pg C y^{-1}) have also been

124   reported from satellite-based products (Antoine *et al.* 1996; Behrenfeld *et al.* 2005; Carr *et al.* 2006; Uitz *et al.*

125   2010) (here we recognize that satellite products may differ in the computed PP components, as noted earlier).

126   Large differences also emerge in the PP trends over the last decades estimated from both the CCI and Oregon

127   State University products (Figure 1B), as well as associated reanalyses (e.g. those of Gregg and Rousseaux, 2019).

128   These differences are strongly impacted by the choice of historical period and the underlying characteristics of

129   the satellite products (e.g. whether they have data-gaps, or not), but the choice of satellite-based PP model does

130   matter. In a recent comparison (Ryan-Keogh 2025) of six satellite-based primary production models applied to a

131   common satellite product (OC-CCI) and a common period (1998-2023), showed that four of them showed

132   declining trends, while the other two showed an increasing trend. Interestingly, the split is along the lines of

133   whether the models incorporated temperature-dependent production parameters, or not. Ryan-Keogh *et al.* (2025)

134   also compared satellite products and outputs of several ecosystem models from the Climate Model

135   Intercomparison Project (CMIP-6), and concluded that, in general, the climate models underestimated the

136   decreasing trends seen in many of the satellite-based models.

137

138
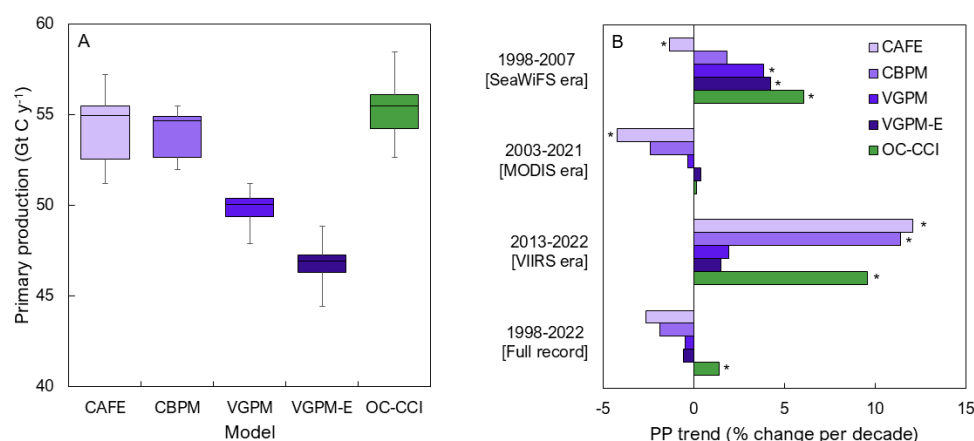
139   **Figure 1.** Global marine PP computed using the satellite-based model of Platt & Sathyendranath (1988) as updated

140   by Sathyendranath *et al.* (2020) and Kulk *et al*. (2020, 2021) with version 6.0 of Ocean Colour Climate Change

141   Initiative (OC-CCI) data as input (in green), compared with openly available time-series data from four other

142   satellite-based primary production models from the Oregon State University Primary Production website

143   (http://orca.science.oregonstate.edu/-npp_products.php) based on single-sensors (Sea-viewing Wide Field-of-

144   view Sensor (SeaWiFS; 1998-2007), Moderate Resolution Imaging Spectroradiometer Aqua (MODIS-Aqua;

145   2003-present), and Visible Infrared Imaging Radiometer Suite (VIIRS; 2013-present)). The panels show the

146   following: A) Global ocean primary production for the five different satellite-based primary production models

147   for the time period between 1998-2022 (i.e., full data record), for all sensors combined; and B) Trends in primary

148   production for the full ocean colour data record and for subsets of the periods during which specific sensors were

149   operational, with stars indicating significant trends ($p < 0.05$), for the five satellite-based primary production

150   models. All latitudes were considered, but coverage at higher latitudes (>70°N and S) is typically poor in satellite

151   data.

152

153

154   Differences in marine PP and its trends are not limited to satellite-based products. Earth System Model

155   intercomparisons show even considerably larger uncertainty than the satellite models for the annual NPP estimate

156   during the (recent past) "historical'' period (i.e., 17-83 Pg C y⁻¹; Bopp *et al.* 2013; Doney *et al.* 2014; Laufkötter

157   *et al.* 2015; Tagliabue *et al.* 2021; see Figure 2), whilst showing weak or no trends over the recent historical period

158   (Kwiatkowski *et al.,* 2020). Ecosystem model uncertainties are even higher in future projections where models

159   disagree even on the sign of change to the year 2100 under the high emission scenario, although most ecosystem

160   models project a decline in global PP. While the uncertainty in annual NPP in the recent past has decreased in the

161   CMIP6 (Coupled Model Intercomparison Project phase 6) ensemble compared with CMIP5, the uncertainty in

162   projected PP trends has increased significantly in the CMIP6 ensemble compared with CMIP5 (Kwiatkowski *et*

163   *al*. 2020). In particular, while the ensemble mean in CMIP5 suggested a significant decrease in PP at the global

164   scale of $-8.06\% \pm 4.83\%$ (where the uncertainties are reported as the inter-model standard deviation), the CMIP6

165   ensemble has a much smaller mean and the standard deviation includes the null hypothesis of no trend (-1.76%

166    $\pm\ 9.01\%$). Frölicher *et al.* (2016) have noted that ecosystem model uncertainties (missing/mis-represented

167   processes, parameter uncertainties) dominated the total uncertainty in the 21st-century projections of PP and their

168   relative importance with respect to scenario uncertainty doesn't decrease with projection lead time. Recent studies

169   have confirmed this, highlighting the role of uncertainty in the representation of key biogeochemical processes,

170   including diazotrophy (Tagliabue *et al.* 2021; Bopp et al., 2022; Doléac *et al.* 2025), bacterial remineralization

171   (Kim et al., 2023) and parameter uncertainty (Jones *et al*. 2024), including in zooplankton grazing rates (Rohr *et*

172   *al.* 2023). Laufkötter *et al.* (2015) concluded that the projected future changes in marine PP are driven by multiple

173   processes, including changes in circulation or mixing, leading to a stronger lateral or vertical loss of biomass;

174   increased aggregation or mortality of phytoplankton; or higher grazing pressure. Laufkötter *et al.* (2015) also

175   noted that temperature-dependent functions of PP and loss terms can affect the direction of change of PP from

176   marine ecosystem models in climate warming scenarios. It should be noted that regional variations in PP are

177   especially sensitive to how model represents these wide range of processes (Dutkiewicz *et al,* 2013), and given

178   the high uncertainty in their model representation, very few of the models agree on the direction of the trend

179   regionally. Furthermore, global models, with their coarse horizontal resolution, will especially struggle to capture

180   coastal processes that enhance PP, which makes them also apt to underestimate global PP.

181

182

183
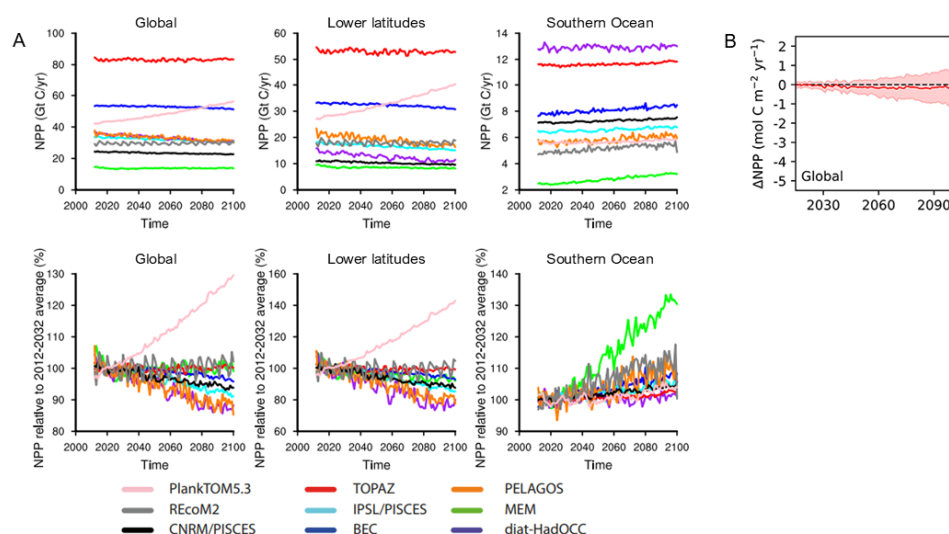
Figure 2. Comparison of NPP from marine ecosystem models in CMIP5 comparison projected to the end of this century under a high emission scenario. A) From Laufkötter et al. (2015) – RCP8.5 (Representative Concentration Pathways 8.5 scenario) with from left to right global values, lower latitudes (30°S-30°N) and Southern Ocean (90-50°S) in Gt C per year (top) and percent (bottom); and B) Global NPP projections from Tagliabue et al. (2021) – SSP5-8.5 (Shared Socio-economic Pathways 8.5 scenario). Note that the magnitude of contemporary annual NPP ranges from less than 20 to more than 80 Pg C y^{-1} in the compilation from Laufkötter et al. (2015). Both analyses showed negative and positive global trends, though most ecosystem models predict decreasing trends towards the year 2100.
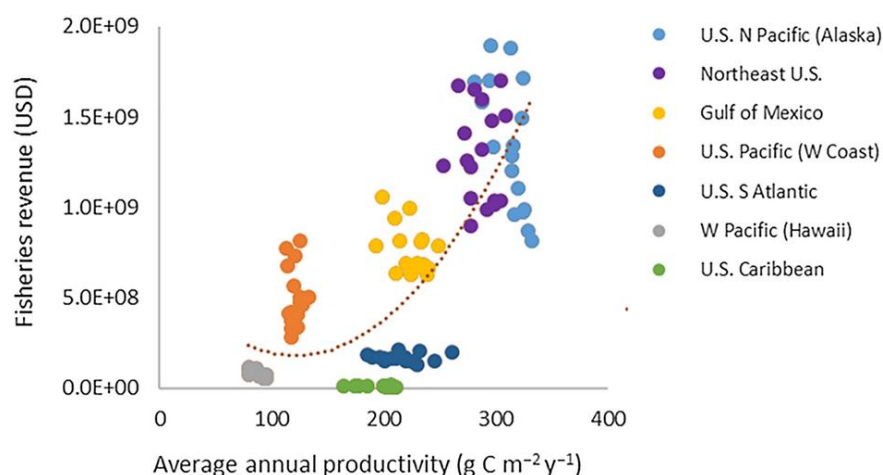
Figure 3. The impact of PP on fisheries. Figure reproduced from Marshak and Link (2021). Individual observations from different coastal regions of the USA are indicated in different colours.

Several studies have also been carried out to compare estimates from ecosystem models with satellite-based products and *in situ* observations, both at global scale (Carr *et al*., 2006, Steinacher *et al.* 2010; Bopp *et al.* 2013; Laufkötter *et al.* 2015; Séférian *et al.* 2020) and at regional scales (Friedrichs *et al.,* 2009, Saba *et al.,* 2010, Lee and Yoo 2016; Doléac *et al.* 2024). In some cases these comparisons (e.g., between ecosystem and satellite-based models) led to better constrained PP projections, e.g., in the tropics, using an emergent constraint approach (Kwiatkowski *et al.,* 2017). However, it is fair to say that overall these comparisons have not led to convergence of model outputs that would reduce the uncertainty of marine PP estimates. All previous works have highlighted large differences between estimates (e.g., varying from <-60% to >60%; Séférian *et al.* 2020), with highly variable spatial patterns (Bopp *et al.* 2013). Tagliabue *et al.* (2021) highlighted the need for stronger constraints on NPP using new approaches that include the growing observational coverage from Biogeochemical-Argo (BGC-Argo) floats (Claustre *et al.* 2020, for an example of this see Arteaga *et al.,* 2022). Such field observations of PP, typically treated as the "truth", are often compared with model outputs to evaluate model performance. However, this type of comparison is confounded by the errors in the field observations themselves, which can be quite high, as well

212   as by the differences in the spatial and temporal scales of the *in situ* observations and the validated models.

213   Furthermore, technologies such as BGC-Argo do not measure PP directly, but infer it from other variables.

214   Given these challenges both in remote sensing and ecosystem modelling, the IPCC has assigned low

215   confidence to current estimates of marine PP and its trends. The reasons cited include uncertainties in production

216   estimates and projections, the short duration of available time series data used in the analyses, and the lack of

217   independent validation (IPCC 2019; Gulev *et al.* 2021; Chapter 2 in IPCC AR6, WG I, 2021). This assessment is

218   of particular concern as it has major implications for ecosystem service provision, mitigation planning, enhancing

219   adaptation and building resilience to climate change (Hewitt *et al*. 2021). These applications often require regional

220   to local information as PP determines spatial variability in ecosystem services such as fisheries (Marshak and

221   Link 2021; see Figure 3), while uncertainties at these scales are further increased compared to the global estimates

222   (Tagliabue *et al.* 2021). Both remote sensing and ecosystem models can, in principle, deliver such regional

223   insights, when used with granularity and resolution needed at the appropriate scales. Reducing uncertainty in

224   models, ideally through a coordinated and internally consistent set of simulations, data and knowledge, would

225   then enable us to discuss downstream services under various climate scenarios and associated risks of tipping

226   points (Jones *et al.* 2024). Such improvements would support climate policy, as well as management decisions

227   pertaining to mitigation and adaptation, at both international and regional levels.

228   We argue here that efforts to reduce uncertainty in estimates and projections of marine PP should include a

229   focus on *investigating model structures and parametrisations*, with the goal of identifying genuine inter-model

230   differences and reconciling apparent differences. In this review, we examine both the sources of differences

231   between satellite-based and ecosystem models, as well as within these two types of models. We argue that there

232   is strong scientific justification for considering how the current model parameterisations could be improved. An

233   avenue to improvement might be to allow parameters that are currently treated as constants (e.g. the A_i parameters

234   from Table 1), to acquire different values at different spatial locations and times. Although this increases the

235   complexity of functional forms used in PP models, we argue that, at least in the less complex PP models (e.g.

236   within satellite models and ecosystem models used in ESMs for climate projections), there are both, good

237   scientific reasons to expect such parameter variations to be present, and to assume that absence of such variations

238   is responsible for the many apparent differences between the current PP models. Parameter variability might be

239   less important for the more complex models with large numbers of phytoplankton types and/or size-classes, but

240   for those models it is still essential to focus on the best possible ways of optimizing the existing constant

241   parameters. In general, we highlight the importance of correct parameterisations that are valid across multiple

242   spatial and temporal scales, and for multiple phytoplankton types. We also discuss the challenges posed by such

243   PP model parametrisations, argue that this is the right time to rise to those challenges, and propose strategies to

244   overcome them. Finally, we discuss uncertainties in marine PP that persist even when improved model

245   parametrisations are adopted.

246

247   **3.   Modelling primary production**

248   In this section, we assess how marine PP is treated in satellite-based and ecosystem models, identifying inter-

249   model differences.

250   It is useful to consider GPP as the product of a biomass-specific production, say P^M, where M is a measure

251   of phytoplankton biomass, multiplied by the biomass itself. In other words:

252
$$P = P^M \times M, \quad (1)$$

253 such that P^M carries all the information on the physiological controls on PP, whereas M accounts for the role of

254 varying phytoplankton concentrations. Since phytoplankton are complex organisms, many options exist for

255 defining biomass, including concentrations of the phytoplankton pigment chlorophyll (B), phytoplankton carbon

256 (C) or nitrogen content. The choice of biomass often depends on practical considerations (such as data availability)

257 or by the study objectives (for example, carbon is an obvious choice in models designed to investigate the

258 biologically mediated carbon cycle in the ocean). Models can also be classified according to which measure of

259 biomass they track as the main currency in the ecosystem.

260 Dimensional analysis suggests that, in its simplest form, P^M can be represented in a canonical form with two

261 parts: a scale factor P_m^M that carries the same dimensions as P^M, and a dimensionless function f_I of the scaled

262 irradiance I_* available for photosynthesis (Platt and Sathyendranath, 1993), where the scaling factor would be a

263 model parameter with the same dimensions as light. Thus, in such a canonical form, P^M can be written as:

264
$$P^M = P_m^M \times f_I(I_*). \quad (2)$$

265 In this form, P_m^M is not strictly constant, but implicitly accounts for the effects of other environmental variables

266 on primary production, such as temperature (T) and nutrients (N), or of changes in species composition. Such

267 dependencies can be made more explicit (removing T and N dependence from P_m^M), such that Equation (1)

268 becomes:

269
$$P^M = P_m^M \times F\big(f_T(T), f_N(N), f_I(I_*)\big). \quad (3)$$

270 The function $F(f_T, f_N, f_I)$ can be specified as a simple product $f_T \times f_N \times f_I$ (e.g., Laufkötter *et al.* 2015; Kishi

271 *et al.* 2006; Vichy *et al.* 2007; Yool *et al.* 2013; Butenschön *et al.* 2016), representing co-limitation by each

272 variable, or it can follow Liebig's law of the minimum (e.g., Gregoire *et al.* 2008; Daewel and Schrum 2013;

273 Radtke *et al.* 2019) where the most limiting resource dictates the growth rate. Note that in Equations 2 and 3, the

274 functions f_i are dimensionless, and that all the dimensions are carried by the scaling factor P_m^M. When models

275 resolve multiple phytoplankton groups or species, then Equation (3) is specified for each group, and their

276 contributions are added to get total PP.
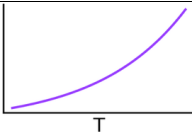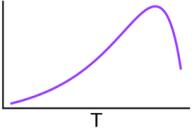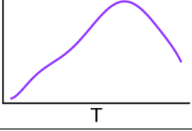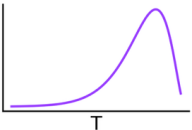
277 Table 1 summarises commonly used functions in PP models that represent the modulating roles of

278 temperature, nutrients and light. When more than one nutrient is considered, additional terms have to be included

279 for each nutrient. Thus, models differ depending on how many environmental factors are included in the model,

280 and on the explicit functional forms selected for each modulating function. Ideally, the combined function F would

281 have values within the [0,1] interval; however, this is often not the case for the temperature f_T function (as

282 illustrated in Table 1).

283 In some cases, it is necessary to track multiple measures of phytoplankton biomass within a model. For

284 example, a unit conversion between chlorophyll and carbon might be needed to make the exponent in the light

285 function (f_I) dimensionless, or it may be that the model tracks more than one currency. Such a conversion may

286 also be needed to transform modelled phytoplankton carbon fields into chlorophyll fields for comparison with

287 satellite-based chlorophyll products. This is typically achieved using a chlorophyll-to-carbon ratio (θ, which

288 varies among phytoplankton and under different environmental conditions and is usually estimated using photo-

289 acclimation models. Commonly used functions in photo-acclimation models are also shown in Table 1. It shows

290 that in those models f_I often takes a more general form and may also contain a dependence on temperature T and

291 nutrients N.
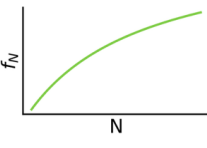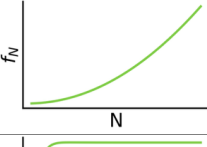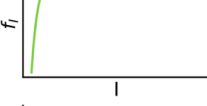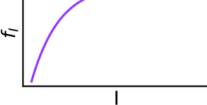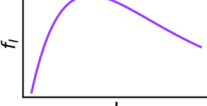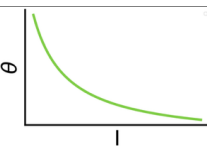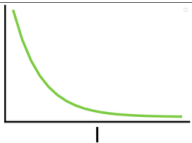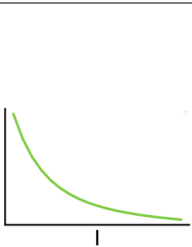
Table 1. The different f_T, f_N, f_I and θ functions used across variety of CMIP and operationally used ecosystem models, as well as satellite models (which however typically do not explicitly use nutrient-limitation function). The ecosystem models explicitly mentioned are Biogeochemical Model for Hypoxic and Benthic Influenced areas (BAHMBI, Gregoire and Soetaert (2010)), Biogeochemical Flux Model (BFM, Vichi et al. 2015), ECOSystem MOdel (ECOSMO, Daewel and Schrum, 2013), European Regional Seas Ecosystem Model (ERSEM, Butenschön *et al.* 2016), Hadley Centre Ocean Carbon Cycle (HadOCC, Toterdell, 2013), Model of Ecosystem Dynamics, Sequestration and Acidification (MEDUSA, Yool *et al.* 2013), Marine Ecosystem Model (MEM, Shigemitsu *et al.* 2012), North-Pacific Ecosystem Model for Understanding Regional Oceanography (NEMURO, Kishi *et al.* 2007), PELAgic biogeochemistry for Global Ocean Simulations (PELAGOS, Vichi *et al.* 2007), Pelagic Interactions Scheme for Carbon and Ecosystem Studies (PISCES, Aumont *et al.* 2015), Carbon, Ocean Biogeochemistry and Lower Trophics (COBALT, Stock *et al.,* 2020, 2025), DARWIN model (Ward et al. 2012). P, h, C and N represent the concentrations of nutrients (such as phosphate, carbon, and nitrogen). A_i and D_i stand for the different model parameters. In photoacclimation models θ is chlorophyll-to-carbon ratio.

Process / Structure	Equation	Description & remarks	Graphical Representation	Examples	Key References
Temperature limitation on photosynthesis	$f_T = e^{A_1 T}$	Exponential temperature dependence on growth rate.	f_T vs T graph (increasing)	BAHMBI, MEDUSA, NEMURO, BFM, PISCES, PELAGOS, COBALT, DARWIN	Eppley (1972)
	$f_T = Q_{10}^{\frac{T-A_2}{A_2}} - Q_{10}^{\frac{T-A_3}{A_4}}$	Phytoplankton growth rate increases initially exponentially, with enzyme inhibition above optimal temperature	f_T vs T graph (peaked)	ERSEM	Blackford *et al.* (2004)
	$f_T = \sum_{i=0}^{7} D_i T^i$	Phytoplankton growth rate is represented as an empirical seventh-order polynomial function, fit to observed data.	f_T vs T graph (peaked)	Vertically Generalised Production Model (VGPM)	Behrenfeld & Falkowski (1997)
	$f_T = A_5 \times e^{A_6 \times T} \times \left(1 - \left(\frac{T-A_7}{A_8}\right)^2\right)$	Function designed to model individual phytoplankton species or types according to their temperature traits, in multi-species models. It has yet to be used routinely in global-scale simulation models, except in a special case of DARWIN.	f_T vs T graph (peaked)	A version of DARWIN	Norberg (2004), Thomas *et al.* (2016); Sauterey *et al.* 2024); Krinos et al. (2025)
	N/A	No explicit temperature dependence is included in the model structure	N/A	ECOSMO, HadOCC	Yumruktepe, Samuelsen, Daewel (2022)
	Empirical assignment	Indirect methods. An example is province-based assignment of parameters	N/A	Satellite P&S, BICEP	Sathyendranath & Platt (1988), Longhurst *et al.* (1995), Sathyendranath

Category	Equation	Description	Graph	Models	References
					et al. (2020), Kulk *et al.* (2020)
N-limitation	$f_N = \left(\frac{\left(\frac{\hat{P}_h}{\hat{C}}\right) - A_9}{A_{10} - A_9} \times \frac{\left(\frac{\hat{N}}{\hat{C}}\right) - A_{11}}{A_{12} - A_{11}}\right)^{0.5}$	Describes nutrient limitation based on internal nutrient quota for phytoplankton cells. Droop model of cell quota. $0 \leq f_N \leq 1$ depends on the instantaneously calculated internal cell C/N and C/P ratios $\left(\frac{\hat{P}}{\hat{C}}, \frac{\hat{N}}{\hat{C}}\right)$ and the maximum C/N and C/P ratios (A_5, A_7), having subtracted the structural content of the cell (A_4, A_6) from each.	N/A	ERSEM PISCES (for iron), DARWIN (quota version)	Droop (1974);
	$f_N = \frac{N}{N + A_{13}}$	Michaelis-Menton Equation. Describes N-limitation as a saturating function of external nutrient concentration, and the half saturation coefficient A_{13} for that nutrient	(graph: f_N vs N, saturating curve)	NEMURO, ECOSMO, BFM, MEDUSA, HadOCC PISCES (for all nutrients except iron), DARWIN (monod version)	Michaelis and Menton (1913), Kovarova-Kovar and Egli (1998), Lee *et al.* (2015)
	$f_N = \frac{(1-f_A) \times A_{14} \times N}{\left(\frac{(1-f_A) \times A_{14}}{f_A \times A_{15}} + N\right)}$, $f_A = \frac{1}{1 + \sqrt{\frac{A_{14} \times N}{A_{15}}}}$	Optimal uptake kinetics	(graph: f_N vs N)	MEM	Smith *et al.* (2009)
Light Limitation	$f_I = I \times e^{1 - A_{16} \times I}$	Photosynthesis rate increases then declines at high light intensities due to photoinhibition.	(graph: f_I vs I)	NEMURO	Steele (1962)
	$f_I = (1 - e^{-A_{17} \times I})$	Photosynthesis follows a light saturation curve with no inhibition at high light levels	(graph: f_I vs I)	Satellite	Platt *et al.* (1980; 1990) Sathyendranath *et al.* (2020); Kulk *et al.* (2020)
	$f_I = (1 - e^{-A_{18} \times I}) \times e^{-A_{19} \times I}$	Photosynthesis follows a light saturation curve with inhibition at high light levels.	(graph: f_I vs I)	BAHBI, MEM	Platt *et al.* (1980)
	$f_I = tanh(A_{20} \times I)$	Model with no photoinhibition. A hyperbolic tangent function is used to simulate light saturation curve.	(graph: f_I vs I)	ECOSMO	Jassby & Platt (1976)
Photo-acclamation	$\theta = \frac{A_{21}}{\left(1 + \frac{A_{21} A_{22} I}{2A_{23}}\right)}$	Photo acclimation model based on the concept of resource allocation, with maximum Chl-to-carbon ratio reached as light approaches zero.	(graph: θ vs I)	ERSEM, BFM, PISCES, PELAGOS, COBALT, DARWIN	Geider *et al.* (1997,1998)

$\theta = 0.022 + (0.045 - 0.022)e^{-3I} - g(N,T)$	The Chl-to-carbon ratio (θ is determined by photoacclimation, and also by nutrient and temperature stress.		CBPM	Westberry *et al.* (2008)
$\theta = \frac{A_{25}}{I \times A_{24}{}^{-1}} \times \left(1 - e^{-(I \times A_{24}{}^{-1})}\right)$	Based on an extended version of Geider *et al.* (1997,1998) photoacclimation model. Uses the exact analytic solution to the Guider et al. (1997) model Jackson *et al.* (2017), extended to to account for spectral light effects (Sathyendranath et al. 2020). It incorporates photo-acclimation effects on the chlorophyll-to-carbon ratio		Satellite	Sathyendranath *et al.* (2020), Jackson *et al.* (2019), Zheng *et al.* (2025)

306

307   In the next two sections, we examine in more detail the variety of ways in which these concepts are implemented

308   in satellite-based and ecosystem models.

309

3.1   Satellite-based models

311   In satellite-based PP models, daily water-column production is calculated as a function of phytoplankton biomass

312   and light available at the sea surface, obtained from ocean-colour remote-sensing observations, coupled with

313   models of photosynthetic response to light. Since the launch of the first ocean-colour satellite, the Coastal Zone

314   Color Scanner (CZCS) in the 1970s, scientists have developed various satellite-based PP models that can be

315   roughly categorised into three classes: 1) Chlorophyll-based models, 2) Absorption-based models, and 3) Carbon-

316   based models (Figure 4). Each of these models differ from each other according to whether they are implemented

317   as linear/non-linear, spectral/non-spectral, vertically-uniform/vertically-non-uniform, or as a combination of these

318   (Platt & Sathyendranath 1993; Sathyendranath & Platt 2007). Further bifurcations occur, depending on whether

319   or not the models are depth-integrated (Friedrichs *et al.* 2009). Most of the satellite-based models do not resolve

320   PP by phytoplankton size classes, or functional types, with some exceptions, such as Uitz *et al.* (2010), Brewin *et*

321   *al.* (2016) and Tao *et al.* (2017).

322   Satellite-based model outputs have been compared against in situ data, both globally and regionally

323   (Friedrichs *et al.* 2009; Saba *et al.* 2010, Lee *et al.* 2015). No clear winners have emerged from these

324   intercomparisons (and perhaps selecting winners was not an objective of the comparisons), and the assignment of

325   model parameters remains one of the biggest sources of uncertainty in estimates of primary production from

326   remote sensing observations (Platt & Sathyendranath 1993; Sathyendranath & Platt 2007, Sathyendranath *et al.*

327   2009; Kulk *et al.* 2020, 2021, Brewin *et al.,* 2023).

328   Interestingly, the types of models described above all converge to the same principles and a common set of

329   parameters (Sathyendranath & Platt 2007; Figure 4). Chlorophyll-based (or available-light or photosynthesis-

330   irradiance) models typically use the parameters of the photosynthesis-irradiance curve, normalised to B, the

331   concentration of chlorophyll-a, i.e., the initial slope (α^B) and the assimilation number (P_m^B) of the light saturation

332   curve, and the photoacclimation parameter ($I_k = P_m^B/\alpha^B$) derived from the other two (Platt *et al.* 1980;

333   Sathyendranath and Platt 2007; Figure 4). Absorption-based (which are also called biomass-independent or

334   inherent-optical-property) models use the realised maximum quantum yield ($\emptyset_m$) and the absorption coefficient

335   of phytoplankton (a_{ph}) (Kiefer & Mitchell 1983, Lee et al. 2015). This model can be shown to be equivalent to

336   the photosynthesis-irradiance models by using the identity $\emptyset_m = \alpha^B/a_{ph}$ (Platt et al. 1988; Sathyendranath and

337   Platt 2007; Figure 4). The key parameter in carbon-based (or growth) models is the growth rate (g), i.e., the rate

338   of change of carbon per unit time normalised to the initial phytoplankton carbon concentration. The chlorophyll-

339   to-carbon ratio (θ) can be used to transform growth models to production models and vice versa (Sathyendranath

340   & Platt 2007; Sathyendranath *et al.* 2009). Thus, the different types of satellite-based primary production models

341   are interchangeable through a common set of parameters: the initial slope (α^B) and assimilation number (P_m^B) of

342   the light saturation curve, the mean specific absorption coefficient of phytoplankton (a_{ph}^*), and the chlorophyll-

343   to-carbon ratio (θ) (Sathyendranath and Platt 2007; Sathyendranath *et al.* 2009). When the light incident at the

344   sea surface exceeds a threshold above which light can damage the photosystems, a photo-inhibition term has to

345   be added to the photosynthesis-irradiance equation (Platt *et al.* 1980). This parameter is often not used in satellite-

346   based models; a sensitivity analysis on a photosynthesis-irradiance model (Platt *et al.* 1990) showed that

347   incorporation of realistic values of the photo-inhibition parameter into the model had only small to negligible

348   effect on computed water-column primary production, which lends some justification to why this term is often

349   ignored. But this is a simplification that can be readily dropped, if new evidence suggests that photo-inhibition

350   could be important at large scales.

351   Spectral models of primary production are designed to capture the wavelength-dependent light penetration

352   underwater, and wavelength-dependent photosynthesis (Sathyendranath and Platt, 1989). In fully-spectral models,

353   the action spectrum of photosynthesis (which describes the wavelength-resolved values of the initial slope α^B is

354   coupled to the light available at corresponding wavelengths for photosynthesis (Sathyendranath & Platt, 1989;

355   Kyewalyanga *et al.,* 1992), such that the product $\alpha^B I$ that appears in non-spectral models has to be replaced by

356   the wavelength integral $\int \alpha^B(\lambda) I(\lambda)\, d\lambda$, where λ represents the wavelength, and the integral is taken over the

357   photosynthetically active range (400-700 nm). The spectral form of the action spectrum closely resembles that of

358   the phytoplankton absorption spectrum (a$_{ph}$) (Sathyendranath *et al.* 1989b; Kyewalyanga *et al.* 1997). Spectral

359   effects are generally considered to be not relevant at saturating light levels. Therefore, if the light available is blue-

360   rich, where action spectrum is maximum, then the coupling between light and photosynthesis would be stronger

361   than if the light were green-rich, where the action spectrum typically goes through a minimum. We know from

362   previous studies that spectral and non-spectral models may differ from each other in a systematic manner

363   (Sathyendranath & Platt 2007), because non-spectral models are not able to account for the covariance (or the

364   lack of it) between spectrally-resolved α^B and a_{ph}. To some extent, the impact of the spectral effects on water-

365   column primary production could be accommodated into non-spectral models by suitably tuning the parameters

366   of non-spectral models (Platt and Sathyendranath 1991). Typically, therefore, one anticipates systematic

367   differences between spectral and non-spectral models of marine primary production, unless model parameters are

368   adjusted to compensate for the difference.

369
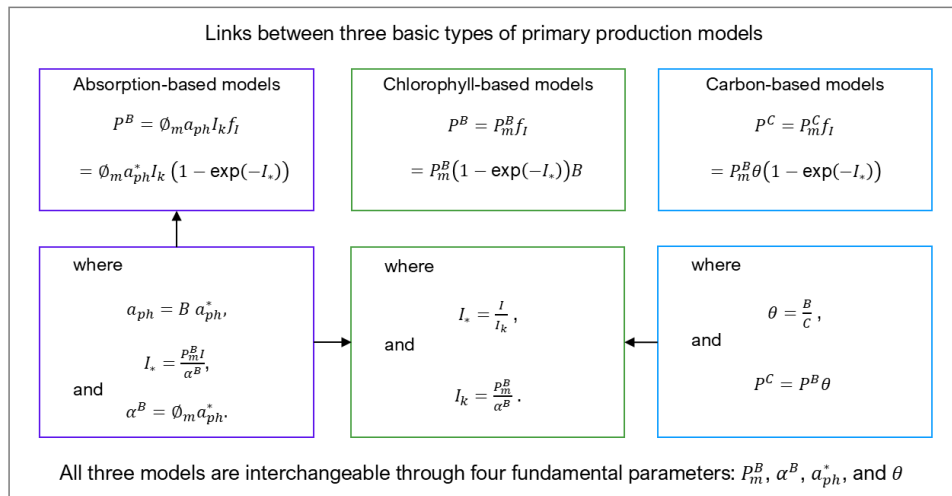
370   **Figure 4.** Phytoplankton absorption-, chlorophyll- and carbon-based primary-production models commonly-used

371   in satellite-based approaches, and the parameter transformations between them. Notations: Primary production

372   (P), light-limitation function (f_I), as in Table 1, assimilation number of the saturation-light curve, or the light

373   saturation parameter (P_m^B), initial slope of the light-saturation curve (α^B), mean absorption coefficient of

374 phytoplankton (a_{ph}), chlorophyll-to-carbon ratio (θ), chlorophyll-specific absorption coefficient of
375 phytoplankton (a_{ph}^*), realised maximum quantum yield of photosynthesis ($\emptyset_m$), photoacclimation parameter of
376 the light-saturation curve (I_k), phytoplankton biomass in chlorophyll-a units (B), normalised irradiance (I_*),
377 irradiance (I), phytoplankton carbon biomass (C), time (t), and growth rate (g). One of the (f_I) functions from
378 Table 1 was selected here for illustrative purposes, but other functions have also been used in the literature. As
379 shown below (Figure 7), numerically, most of the (f_I) functions are almost identical to each other, unless photo-
380 inhibition is introduced. Currently, remote-sensing-based primary-production models do not incorporate the
381 photo-inhibition term.
382
383 **3.2 Ecosystem models**
384 Ecosystem models differ greatly in their complexity, ranging from simple, three-component Nutrient-
385 Phytoplankton-Zooplankton (NPZ) models (Fasham *et al.* 1990; Steele and Henderson 1992; Franks, 2002;
386 Gentleman, 2002) to highly complex ones with hundreds of ecosystem components (e.g., Dutkiewicz *et al.*, 2020,
387 Fennel et al. 2022). Some models use a single nutrient (usually nitrogen, or carbon) as the model currency,
388 assuming a fixed stoichiometry (relationship between biogeochemically-important elements), whereas other
389 models allow for dynamically resolved stoichiometry within f_N. In this section, we focus primarily (but not
390 exclusively) on marine ecosystem models (here used interchangeably with "`marine biogeochemical models''")
391 that participate in the Climate Model Intercomparison Project (CMIP) (e.g., Laufkotter et al. 2015; Kwiatkowski
392 et al. 2020), as well as regional ecosystem models that are run operationally by forecasting centres (e.g., Fennel
393 et al. 2019) for regional climate projections. In these models, primary production is usually estimated along the
394 lines of equations 2 and 3, where primary production (P) is calculated by multiplying the phytoplankton biomass
395 (usually carbon) by its reference growth rate g), modulated typically by the three functions, f_T, f_N and f_L.
396   There are also many similarities across the ecosystem models that go beyond the functional form of Equation
397 (2), and a few common approaches can be identified in the equations used to express the functions f_T, f_N and f_L,
398 (Table 1). For instance, f_T is typically described through an exponential function (originating from Eppley et al.
399 1971; e.g., see Laufkotter et al. 2015), that might include inhibition at temperatures much higher than those
400 optimal for the species' growth (e.g., Norberg 2004; Butenschön et al. 2016, Dutkiewicz et al., 2020a), which is
401 based on Q10, a measure of the sensitivity of photosynthesis to temperature. However, most models resolve groups
402 of phytoplankton (e.g. diatoms) rather than individual species, and they do not have temperature inhibition
403 assuming that there is a spectrum of diatoms that have optima across the full temperature range (see e.g. Anderson
404 et al 2020). Furthermore, some models do not have explicit PP temperature dependence at all (e.g., Daewel and
405 Schrum 2013). When multiple nutrients are considered, the f_N function is typically formulated to use Liebig's law
406 of minimum to combine their effects on PP, and is often based either on cell quota of nutrients within the cells
407 (Droop 1974), or on the concentrations of the nutrients in the medium (Michaelis and Menten 1913). In some
408 cases (e.g., Shigemitsu et al. 2012), f_N is based on the optimal uptake kinetics (Smith et al. 2009), which allows
409 for parameters in the Michaelis-Menten equation to vary (Table 1). A variety of equations are currently in use to
410 describe the light-dependence function (f_I, see Table 1) in ecosystem models, including those from Platt et al.
411 (1980), Steele (1962), and Jassby and Platt (1976), some of which account for the effect of photo-inhibition at
412 high light, whilst others do not. Furthermore, many of the ecosystem models also include photoacclimation, either
413 as part of the f_I function, or as an additional term, mostly following the model of Geider et al. (1997,1998).

414   Other significant differences across ecosystem photosynthesis models include the number of phytoplankton

415   functional types and size-classes represented, the number of limiting nutrients included (and the types of equations

416   selected to represent the role of each nutrient), and the number of wavebands considered in representation of

417   irradiance (the level to which light is spectrally and directionally resolved, e.g., see Platt and Sathyendranath 1991,

418   Dutkiewicz et al. 2015, Gregg & Rousseaux, 2016). Practically all ecosystem models include nitrogen limitation.

419   But iron limitation is also considered important, as is silica limitation, especially in those models that include

420   diatoms as a phytoplankton class. Phosphate limitation becomes important as well, in particular when dealing

421   with nitrogen-fixing organisms. Another fundamental difference lies in the representation of the production and

422   remineralisation of particulate and dissolved organic matter which are included in the models as explicit or implicit

423   processes, affecting the model parametrisations up to the formulation of gross primary production which may or

424   may not include exudation (e.g. Butenschön et al 2016, Vichi et al. 2007, Wu et al. 2021).

425

3.3   Comparison of satellite-based and ecosystem models

427   Satellite-based and ecosystem models for estimating ocean PP have some similarities, but also key distinctions

428   (see Figure 5, also IOCCG 2020). Model parameter assignment provides one clear perspective on a difference

429   between the two types of models. For example, parameters associated with PP models in the satellite-based

430   approach of Platt and Sathyendranath (1988), Kulk et al. (2020) and Sathyendranath *et al.* (2020) are established

431   from field observations, whereas ecosystem model parameters are typically estimated using information from

432   laboratory experiments conducted under controlled conditions, followed by tuning the model towards the available

433   observations. But here also, the distinction is not total: for example, the carbon-based production model of

434   Behrenfeld *et al.* (2005) relies on culture measurements to establish growth rate and carbon-to-chlorophyll ratio.

435   The satellite-based models that do not have explicit nutrient and temperature dependencies, inherently contain

436   those dependencies in the model parameter values, which are allowed to vary across biogeographical provinces

437   and seasons (e.g., see Figure 6; for model described by Longhurst *et al.* 1995 as updated by Sathyendranath *et al.*

438   2020 and Kulk *et al*. 2020, 2021), representing different nutrient and temperature limiting environments.

439   Ecosystem models typically represent the nutrient and temperature limitation explicitly, with different parameters

440   assigned to each plankton group. Another difference in parameterisation is that many ecosystem models use

441   maximum carbon or nitrogen-specific production rate under optimal conditions as a model parameter and carbon

442   or nutrient biomass is then used to estimate primary production (Figure 5). While carbon-based satellite algorithms

443   for primary production are similar to ecosystem models in this respect, other satellite models rely on bio-optical

444   properties such as chlorophyll concentration or phytoplankton absorption coefficient as the state variable. Some

445   ecosystem models also include a photo-inhibition term, to represent the reduction in photosynthesis under high

446   light intensities, whereas satellite-based models typically account only for the saturating response to light without

447   including photoinhibition. Another process linked to photosynthesis, photo-acclimation, is generally addressed by

448   both approaches and though there are differences, variations of the Geider *et al.* (1997, 1998) models are now

449   common to both satellite-based and ecosystem models.

450   Finally, the ecosystem models are able to compute depth-resolved PP, as is the case for the satellite-based

451   method proposed by Platt and Sathyendranath (1988), whereas some other satellite-based models are designed to

452   yield vertically integrated production (e.g., Behrenfeld and Falkowski 1997).

453
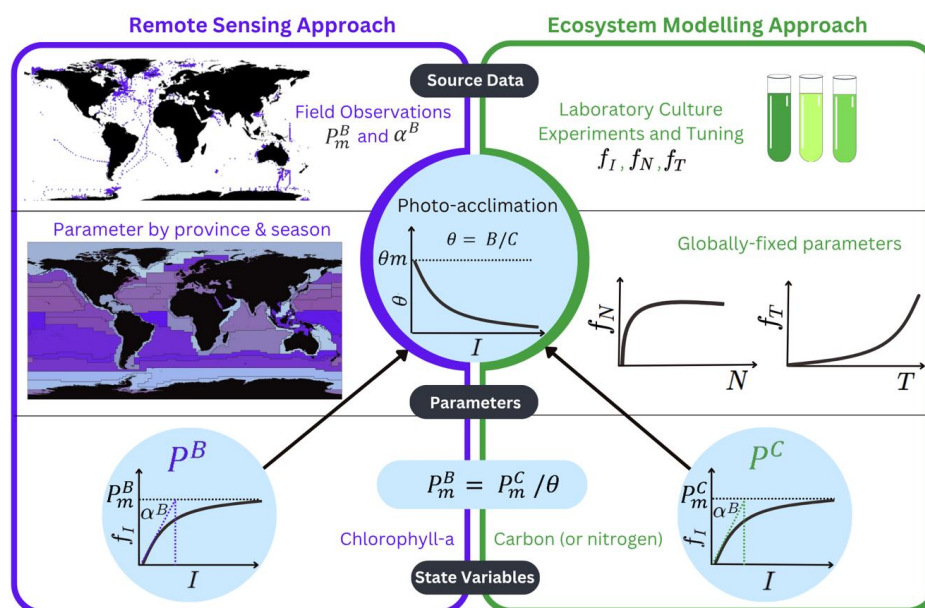
Figure 5. Comparison of satellite remote sensing (left) and ecosystem modelling (right) approaches to computing marine primary production, and where they interact (light blue) through the photo-acclimation model which is essential to enable comparison between the models. I = Light, N = Nutrient, T=Temperature. It should be noted that although carbon, or nitrogen, are the most common currency used by the ecosystem models, there are also ecosystem models which use chlorophyll-a as the currency.

459

Thus, the differences between satellite-based and ecosystem-based models of primary production are not clear cut. All satellite-based models are data-rich, in the sense that they are designed to exploit satellite observations, typically with global coverage and nominal daily repeat frequency. Some use culture data as auxiliary information; others rely on in situ field observations. Ecosystem models, on the other hand, tend to be data-sparse; even when operated in data assimilation mode, only a fraction of the modelled ecosystem compartments or fluxes are usually constrained by assimilation. The constraints imposed by satellite data availability limit the processes and variables that can be estimated, whereas ecosystem models tend to be rich in outputs they provide.

Platt and Sathyendranath (1997) proposed a hierarchy of primary production models (Figure 7). Almost all the types of models in this hierarchical classification, with the exception of linear models and purely statistical models, are represented in PP models under discussion in this paper. With the exception of absorbed-light models that are in use in satellite-based models, but not in ecosystem models, the different classes of models are common to both. In this regard, the diversity of models within satellite-based or ecosystem-based approaches is no smaller than across those two groups of models.

473

474
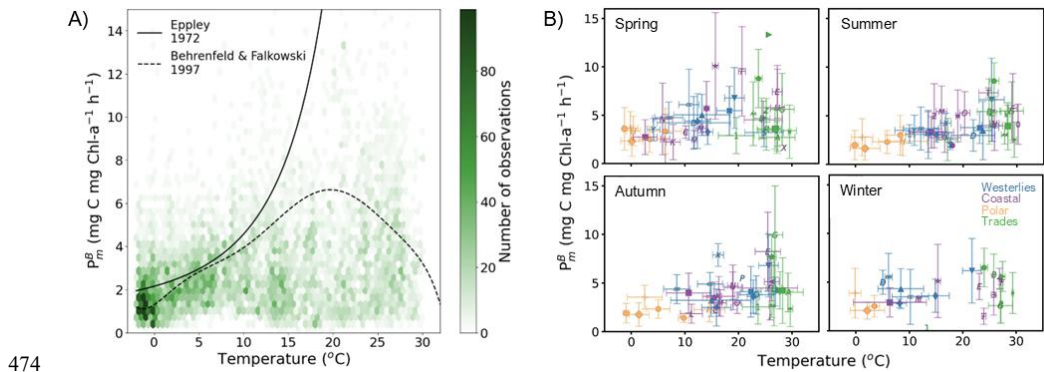
Figure 6. Variability in the photosynthesis-irradiance parameter P_m^B in the ocean. A) Parameter values from a global in situ dataset (Bouman et al. 2018; Kulk et al. 2020) plotted as a function of temperature. Two commonly-used temperature-dependent equations (Eppley 1972; Behrenfeld and Falkowski 1997) of this parameter are also shown. B) The same data sorted according to ecological provinces of Longhurst (2007) and according to season, with colours representing four different oceanic biomes (Longhurst 2007), showing that some structure and pattern emerge when the data are organised according to oceanic biomes and to a smaller degree seasons.

481
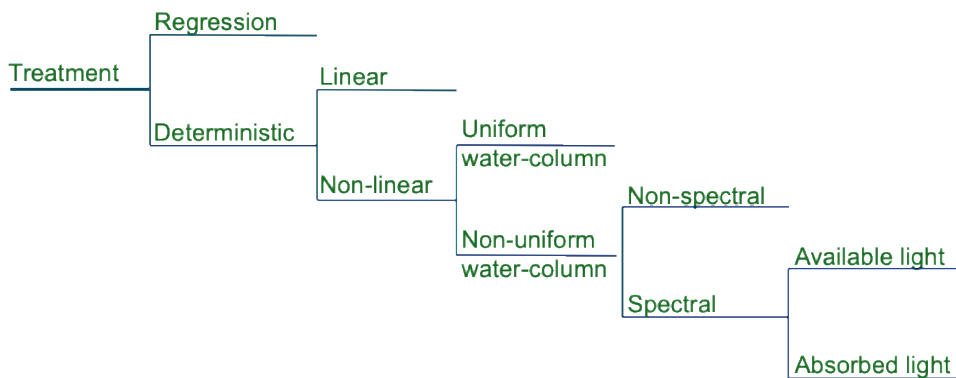
Figure 7. Hierarchy of primary production models. The models get more complete (and more complex), as we go from left to right, and from the upper to the lower limb of each branch.

484

485

486 **4.   How similar are the different primary production models?**

487 Platt and Sathyendranath (1993) showed that we can anticipate systematic biases between satellite-based models
488 that are structured differently, and we can numerically predict under what conditions the biases will manifest
489 themselves. For example, linear and non-linear models are expected to behave similarly under low-light levels
490 but to diverge as light levels increase. However, they showed that when PP models have similar structures, it is
491 possible to reduce all of them to a common, canonical form, revealing that apparently-different model types
492 (available light models, absorbed light models, chlorophyll-based or carbon-based models) become equivalent
493 when implemented with comparable model parameter values (Platt and Sathyendranath 1993; Sathyendranath and

494   Platt 2007; Sathyendranath *et al.* 2020). Such comparisons also reveal systematic biases between spectral and

495   non-spectral models of PP, arising from spectral effects in both underwater light penetration and phytoplankton

496   light utilisation. It was demonstrated that biases between spectral and non-spectral PP models can be minimised

497   by tuning the diffuse attenuation coefficient of downwelling irradiance, which determines the rate of change of

498   available light with depth (Platt and Sathyendranath 1991; Kyewalyanga *et al.* 1992). Similarly, Kovač *et al.*

499   (2016a) demonstrated that a locally tuned non-spectral model, with adjusted values of photosynthesis parameters,

500   can outperform a spectral model, without locally tuned values of photosynthesis parameters. Such comparisons

501   bring to the fore the importance of parameter assessment, assignment, and evaluation to understand model

502   performances, uncertainties and divergences, which is at the core of this review.

503   To illustrate the point, let us focus, for example, on the light function (f_I), which takes a wide range of forms

504   in the literature (see Table 1). Even though the functional forms cannot be analytically transformed into each other

505   (they are mathematically different), numerically they could still be very close to each other, in the sense that they

506   can all fit the same observations similarly well when the parameters are chosen appropriately, for the range of

507   light values commonly encountered at sea (Kovač *et al.,* 2017). These different forms split into two classes: one

508   that includes photo-inhibition and the other that does not (Amirian et al., 2025). Figure 8 shows that the f_I models

509   without photo-inhibition (Webb *et al*. 1974; Jassby and Platt 1976; Smith 1936) are all practically identical to

510   each other for equivalent parameter values and are therefore basically indistinguishable from each other. It should

511   also be noted that the Webb *et al.* (1974) model is a special case of the Platt *et al.* (1980) model for the case of

512   zero photo-inhibition. The f_I model that stands out is the one of Steele (1962), which struggles to match the other

513   f_I models under low light conditions. However, when photo-inhibition is important, the f_I model of Platt *et al*.

514   (1980) can again nicely coincide with Steele (1962) for a suitable combination of their parameter values. What

515   we learn from Figure 8 is that a lot of the diversity in f_I models is only apparent, as the diversity can be eliminated

516   via model parametrisation.

517
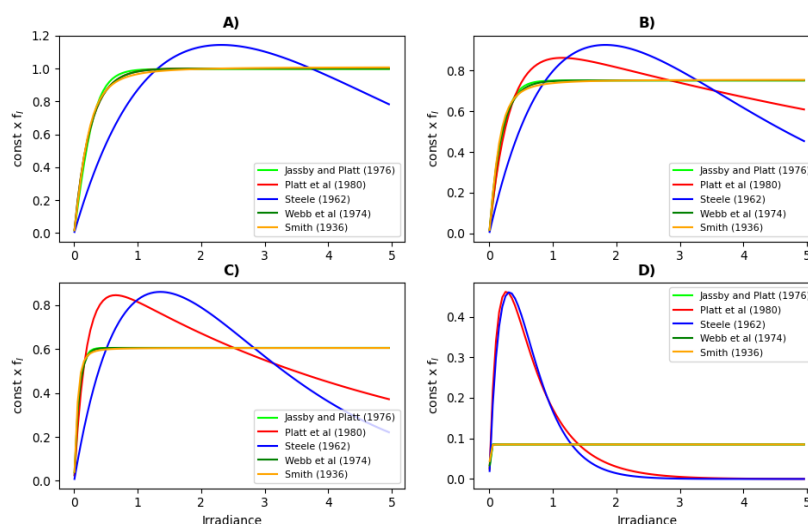
518

519 **Figure 8.** Comparing the functional forms of four f_I models in different regimes. Since only the functional forms
520 are compared, the x and y axes do not necessarily represent realistic values of irradiance and f_I, or alternatively
521 the units in which these variables are expressed are not relevant. The Figure shows the degree to which the five
522 different models can be "tuned" to each other through fitting their parameters in a suitable way. The functional
523 forms for the f_I models are introduced in Tab.1, except the model by Webb *et al.* (1974), which is a special case
524 of Platt *et al.* (1980) for zero photoinhibition (setting $A_{14} = 0$, see Tab.1). However, unlike Tab.1, we include
525 here into the free f_I parameters also a multiplicative constant (hence what is plotted here is const x f_I), which can
526 be always absorbed into the P_m^M parameter of equations (2-3). The different panels A-D show cases of increasing
527 photoinhibition as modelled by the most complex Platt *et al.* (1980) model (A is the lowest, D the highest), with
528 the other models calibrated to best fit the curve corresponding to Platt *et al.* (1980). We see that the five models
529 essentially split into two families, each representing well a limiting case of either no photoinhibition (Jassby and
530 Platt 1976, Webb *et al*. 1974, Smith 1936), or very high photoinhibition (Steele 1962).

531

532   In general, PP models are designed to represent limitations to phytoplankton growth (whether from light,
533 nutrients or temperature) under different environmental conditions. These models have the potential to be
534 generalised to deal with additional external conditions (which may not be explicitly included in the model) by
535 incorporating spatially and temporally variable parameter values. This flexibility allows models to account for the
536 diversity of plankton and the processes responsible for their dynamics, which are not explicitly represented in
537 current models. Representing the full diversity of planktonic species is not feasible due to lack of understanding
538 and computational demand, which is why models typically rely on the use of plankton classes to represent
539 aggregations of multiple species based on shared characteristics or traits, such as body size, life strategies and
540 behaviours. This approach captures at best the average or most typical behaviour of each class (e.g., Anderson
541 2020; Ratnarajah *et al.* 2023). When aggregating species according to their physiological and functional traits and
542 behavioural patterns into a pre-defined number of modelled classes, fixed values are assigned to model parameters
543 within each aggregated class. For ecosystem models, many of these parameters have assigned values on the basis
544 of laboratory or mesocosm experiments (Geider *et al.* 1998; Schartau et al. 2017; Ratnarajah *et al.* 2023), often
545 focusing on a small number of carefully-selected species, far from capturing the full diversity of organisms or
546 their responses and behaviours that might be expected in the natural environment across large spatio-temporal
547 scales (Geider *et al.* 1998; Schartau *et al.* 2017; Ratnarajah *et al.* 2023). In contrast, in the natural environment,
548 we can expect parameters to vary in time and space, reflecting both changes in the governing conditions and in
549 the unresolved functional diversity in the makeup of planktonic communities (Schartau *et al.* 2017). Such
550 parameter variability can be observed in model calibration experiments (e.g., Leeds *et al.* 2011; Mattern *et al*.
551 2012, 2014), including those using data assimilation to estimate model parameters jointly with the model state
552 (e.g., Pastres *et al.* 2003; Tijputra *et al.* 2007; Roy *et al.* 2012; Doron *et al.* 2013; Simon *et al.* 2015; Gharamti *et
553 al.* 2017a,b; Skákala *et al.* 2024).
554   A simple illustration of how parameter variability emerges from aggregating species in classes is provided
555 in Figure 9. Although many models differ in the number of phytoplankton classes they resolve, for each
556 phytoplankton class they typically use the same functional form to describe photosynthesis, with total
557 phytoplankton primary production corresponding to the sum of contributions across all classes. Figure 8
558 demonstrates that models with different numbers of classes become equivalent in their description of total PP,

559 provided that the parameters in models with fewer classes are allowed to vary in space and time. In such way,

560 spatio-temporal parameter variations effectively capture the influence of unresolved diversity in plankton

561 community structure in models with fewer plankton classes. The spatio-temporal model parameter variations are

562 then a consequence of models' inability to sufficiently resolve plankton species, which also means that such

563 parameter variability is expected to be especially relevant for simpler models (e.g. ecosystem models typically

564 used in ESMs). We acknowledge that the most complex models currently in use (e.g. DARWIN, see Ward *et al.,*

565 2012, Dutkiewicz *et al.,* 2020a) have less reason to adopt spatio-temporally variable parameters, but these models

566 are typically too computationally expensive to be run as part of ESMs in long-term ensemble-based climate

567 projections and even as complex as they are, they still represent a fraction of the real-world diversity. On the

568 other hand, as the models get more complex by incorporating more ecosystem compartments, the challenge shifts

569 to calibrating large numbers of parameters to describe the functions of each of the model components.

570

571
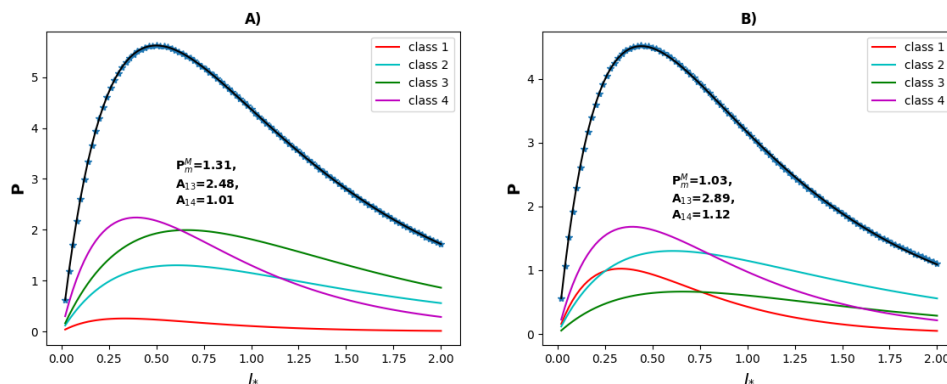
572 **Figure 9.** A simple illustration of how unresolved phytoplankton community structure can lead to parameter

573 variability. In both panels, we plot PP expressed as $P = P_m^M \cdot f_I(I_*) \cdot M$ with functional form f_I corresponding to

574 the Platt *et al.* (1980) model (see Tab.1). As in Fig.6, ranges of irradiance, I_*, and PP values are chosen arbitrarily,

575 purely to demonstrate the essential point made in section 2. Four phytoplankton classes are plotted each with

576 different P_m^M, A_{13}, A_{14} parameters. The dark blue dots are obtained by summing up the PP across the four classes

577 (this corresponds to PP of total phytoplankton) and the dark blue line is the fit of the points with the same

578 functional form used for the four phytoplankton classes assuming the total phytoplankton concentration is the sum

579 of the concentrations of the four classes. The two panels show two situations where the same total phytoplankton

580 concentration is distributed into classes in different ways (the phytoplankton community structure changes). We

581 can see that if we did not resolve the four classes, we could still use the Platt *et al.* (1980) model (including

582 photoinhibition) for the total phytoplankton, but P_m^M, A_{13}, A_{14}, parameters would vary depending on the

583 (unresolved) variations of the phytoplankton community structure.

584

585 **5.   A way forward**

586 Together, these considerations suggest that investigating parameter assignment and parameter variability may be

587 an important route to understand and potentially reduce many of the apparent differences between marine PP

588 models, and hence in the estimated magnitudes of production. Investigation into the role of parameters should be

589 followed by a consistent calibration against the same observational data. To estimate spatially and temporally
590 varying parameters in ecosystem models, data assimilation can provide a natural tool for model calibration (e.g.,
591 Tjiputra *et al.,* 2007; Singh *et al.,* 2025). However, introducing spatio-temporally variable (or too many constant)
592 parameters commes with its own challenges. For example, allowing the (often many) model parameters to vary
593 substantially increases model flexibility at the risk of overfitting to observations, particularly if the number of
594 model parameters is large or observational data are insufficient. Overfitting may reduce the model ability in
595 predicting new phenomena, including future climate-driven changes. It is therefore essential that introducing
596 variable parameters takes into account such risks and ensures that reasonable assumptions are made to simplify
597 the parameter calibration task. These assumptions would ensure that model calibration is sufficiently constrained,
598 so that there are sufficient observations per each calibrated model parameter value. For example, only a carefully
599 selected subset of parameters may be calibrated, based on their relevance for primary production (established, for
600 example, through sensitivity analysis, e.g. Ciavatta *et al.* 2025) and lack of correlations with other model
601 parameters.

602   A key consideration when exploring variable parameters is the spatial and temporal scales at which they
603 might vary. For example, it would be important to establish whether seasonal climatological variability in
604 parameters alone can capture observed patterns, implying that both inter-annual and sub-seasonal variability could
605 be negligible. If so, this would relax the requirement on the volumes of observational data needed for the
606 calibration. Hypotheses about temporal variability scales for model parameters can be tested using long time-
607 series of measurements at specific stations, such as the Bermuda Atlantic Time-series Study and the Hawaii Ocean
608 Time-series, both of which present seasonal cycles in photosynthesis parameters (Kovač *et al.,* 2016b: Kovač *et*
609 *al.,* 2018). Another key question is whether parameters vary over fine spatial scales or maintain coherence over
610 large scales, such as ocean biomes or Longhurst provinces (Longhurst 2007). Preliminary evidence suggests that,
611 at least for the global-scale applications, ecological provinces according to Longhurst might provide an
612 appropriate template for mapping parameters (see Figure 6B), and that monthly or seasonal time scales might be
613 appropriate for modelling variability in photosynthesis-irradiance parameters (Britten *et al.* 2025). If province-
614 based approaches emerge as viable candidates, it would be desirable to avoid sharp discontinuities in parameter
615 values at province boundaries, which might require incorporation of smoothing methods to make inter-province
616 changes seamless. Moreover, it is essential that model parameter calibration does not compensate for unrelated
617 spatio-temporally varying model biases, such as those arising from external forcings or other ecosystem model
618 constraints (e.g., boundary conditions). For example, given the importance of underlying physical processes,
619 caution should be applied when calibrating parameters in ecosystem models to reproduce the observed PP because
620 the model simulation could improve, but for the wrong reasons. Singh *et al.* (2025) illustrate that ecosystem
621 parameters in global ocean biogeochemical models are likely calibrated to compensate for biases in their physics
622 (see also Loptien and Dietze, 2019). To avoid mixing different sources of ecosystem model errors, parameters
623 should be ideally estimated jointly with the model state, e.g., using joint parameter-state data assimilation
624 techniques (Schartau *et al*. 2017). Finally, existing knowledge of acceptable ranges of parameter values needs to
625 be incorporated into the calibration process to prevent parameters from acquiring unrealistic values.

626   Since parameter spatio-temporal variability results from poorly resolved species types or ecosystem
627 processes, interesting insights into its scale and patterns can be also obtained by comparing models of different
628 complexity. For example, high complexity models (such as the DARWIN ecosystem model) could be used in

629 some cases to deduce parameter variability of simpler models, or even possibly help inform spatio-temporally

630 varying parameter calibration of those models. Comparison studies across models of different complexity would

631 be desirable in this case (for some examples see Friedrichs *et al.*, 2007, Xiao and Friedrichs, 2014).

632   It should be noted that even after successfully overcoming the challenges associated with spatio-temporal

633 parameter calibration, significant PP uncertainty is likely to remain in both historical estimates and future

634 projections. For satellite-based models, this uncertainty is mostly driven by inherent observational biases, e.g.,

635 gaps in data due to cloud cover or adverse viewing geometry, or inaccuracies in satellite products associated with

636 bio-optical conditions in water. For ecosystem models, additional sources of uncertainty include the forcing data

637 and the physical model driving biogeochemical processes, e.g., its vertical and horizontal resolution, and its ability

638 to represent currents and mixing responsible for nutrient supply and export of organic material. Further constraints

639 are inherent to ecosystem models themselves. Traditionally, plankton are divided into phototrophic phytoplankton

640 and phagotrophic zooplankton. However, recent research emphasises ubiquitous presence of mixotrophy in the

641 global ocean (Mitra *et al.* 2023), which not only differs in its physiology and ecological role, but can interact with

642 other types of plankton in complex ways (Flynn and Mitra 2023). Despite certain commonality in their approach

643 to modelling primary production, as discussed above, models differ significantly in their approaches to represent

644 various biogeochemical processes such as grazing and associated fluxes, deposition of organic matter and its

645 remineralisation. For many of those processes (e.g. zooplankton grazing), lack of data, variability and high

646 uncertainty of available data, are a major issue. Focusing on biological ocean carbon storage, Henson *et al.* (2024)

647 identified key areas where improved understanding of processes is required to support future modelling efforts.

648 For PP, the processes that were ranked highest were: resource limitation for growth, nitrogen fixation, zooplankton

649 processes and phytoplankton loss processes. Current ecosystem models differ considerably in their formulation

650 and parameterisation of these processes, contributing to uncertainties in model outcomes. Moreover, nitrogen-

651 fixation is often not included in these models. Even when these key processes are included, spatial parameter

652 estimation through assimilating observed state variables (such as water column nutrients and oxygen) in ocean

653 biogeochemical models does not necessarily lead to an improved estimate of primary production, suggesting that

654 current ecosystem model parameterizations may still be oversimplified compared to the real world (Singh *et al.,*

655 2025). The time is right to address the problem of parameter estimation in PP models, both for ecosystem models

656 and satellite-based models. Novel and rapidly expanding observations such as BGC Argo profiles, other types of

657 autonomous data collected by in-water vehicles and also large marine mammals (Chai *et al.* 2020; Claustre *et al.*

658 2020) have been providing large volumes of biological and bio-optical data that complements in situ data from

659 long time series stations and could be harnessed for this purpose (Figure 10). Complementary observations from

660 satellite remote sensing, now available over multiple decades and merged into climate-quality, consistent data

661 streams (e.g., Sathyendranath *et al.* 2019), is another rich data source, along with novel satellite products from

662 emerging capabilities such as geostationary, lidar, cubesat and hyperspectral data. When these are combined with

663 more traditional in situ platforms, including long-term gridded climatology from sources such as World Ocean

664 Atlas (WOA, e.g., Garcia *et al.*), there is already enough data to support a suitably-constrained spatio-temporally

665 varying parameter calibration. This opportunity is further enhanced by new advances in artificial intelligence and

666 machine learning, giving us an historically unprecedented capability to exploit these large and growing datasets

667 and address long-standing questions about marine PP.

668   However, crucial to this endeavour would be a clear focus on data quality, and on data validation, following
669   community-wide accepted protocols and reliable uncertainty characterization. Moreover, some regions, such as
670   sea-ice margins, coastal margins, and high latitudes in winter, which are often regions experiencing long-term
671   rapid changes and include some of the most productive areas of the global ocean, also tend to be regions that are
672   difficult to observe, and hence suffer from sparse data coverage. More observations are needed in such locations
673   to understand how model parameters might evolve in the future. Even if constrained spatio-temporally varying
674   calibration is possible in these regions with the available data-sets, the importance of further investing in data
675   quantity and quality cannot be overemphasized.
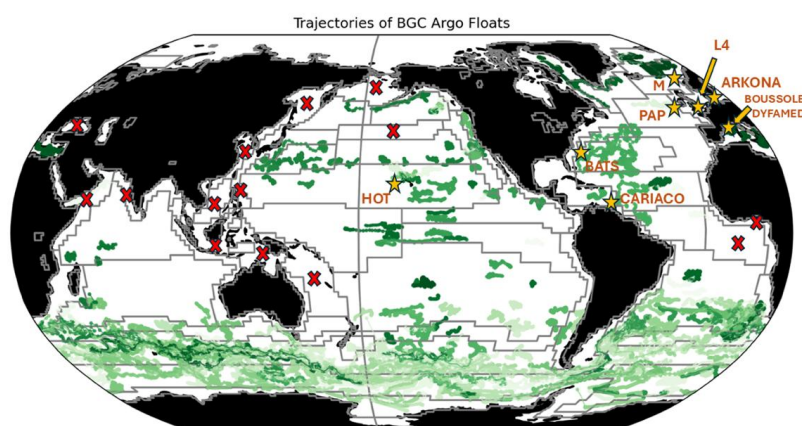
676

677   **Figure 10.** The global in situ data available for model calibration. The boundaries show ecological provinces
678   according to Longhurst (2007). BGC-Argo float trajectories are shown in shades of green, providing sufficiently
679   long time-series (since 2008) for calibration. Orange stars mark in situ time series stations with sufficiently long
680   time-series records that can also be used for model calibration. The red crosses mark provinces without sufficient
681   BGC-Argo data or in situ stations, where the models will need to rely solely on satellite records and compilations
682   of in situ observations, such as the World Ocean Atlas.

683

684   **6.   Conclusions**

685   We have argued that, given the growing abundance of observations from diverse platforms, such as satellites and
686   BGC-Argo, combined with rapidly advancing capabilities in ensemble data assimilation techniques and artificial
687   intelligence, the time has now come to address explicitly the importance of parameter assignment in primary
688   production models, and in exploring the spatial and temporal variability in the parameters. We have theoretically
689   justified why such parameter variability is to be expected both in the satellite-based models (where some models
690   already employ variable parameters albeit in a simple fashion) and ecosystem models (where such assignment is
691   still quite rare), at least unless the models are of very high complexity. In the case of primary production, the
692   number of phytoplankton classes that are included in the model is a key differentiator of the model complexity.
693   Relatively simpler models, such as the ecosystem models used as part of ESMs in climate projections, have limited
694   capability to resolve phytoplankton communities. For such models, spatio-temporally varying parameters could
695   provide a means to account for the unresolved phytoplankton variability and processes.

696   Spatio-temporally variable parameter calibration can shed light on the sources of differences between lower-
697   medium complexity ecosystem models used in ESMs and satellite-based primary-production models. Since
698   variable parameters can capture, in a simple manner, processes or conditions that are not explicitly included in a
699   model, analysing the drivers of parameter variability could help identify how best to overcome current model
700   drawbacks. Furthermore, providing those models with spatio-temporally varying parameters could remove many
701   apparent differences between models, both potentially reducing the spatial and temporal biases in model parameter
702   calibration and enabling the simpler ecosystem models to represent better the effects of unresolved processes or
703   plankton classes. We argue that this could reduce the existing high uncertainty both in historical estimates and
704   future projections of marine primary production. Due to the importance of primary production for climate
705   research, improving its prediction can have a major impact on both climate mitigation and adaptation planning.

706   In the context of our climate, we need to understand how marine ecosystems in general, and phytoplankton
707   in particular, respond to change. Three types of changes need investigation: changes in (i) phytoplankton biomass
708   (whether they be measured as chlorophyll, carbon or nitrogen concentration, or all of them); (ii) the rates of
709   biological processes, with marine primary production being a key process in the global carbon cycle; and (iii)
710   community structure. The first of these can be addressed using fixed model parameters, but we would not know
711   if the effect of variable parameters could have important impacts, if it were not part of the investigation. The
712   second and third objectives both are intimately linked to parameter variability, with the third one in particular
713   calling for resolution of parameter variability at the level of major components of the phytoplankton community.

714   For many decades, we have relied on comparisons and analyses of (both satellite and ecosystem) model
715   outputs for insights into model performance, and for identifying the way forward. It is now time to shift the
716   emphasis toward understanding the behaviour of model parameters, across models, across multiple phytoplankton
717   types, and across multiple spatial and temporal scales. This focus has the potential to reduce uncertainties, unify
718   divergent model results, and provide a stronger foundation for predicting marine primary production under
719   changing climatic conditions.

720   **Code/data availability**: No new data, or code published in this paper.

721   **Author contributions:** JS organized the writing of the manuscript with substantial input by SS, and all the
722   authors contributed ideas, text and Figures.

723   **Competing interests**: The authors declare that they have no conflict of interest.

724

725   **Acknowledgments:** This work was funded by the European Space Agency (ESA) project Climate and Marine
726   Production (CAMP). JS, YA, GL, DB also acknowledge UK National Capability funding Atlantic Climate and
727   Environment Strategic Science (Atlantis). RJWB was supported by a UK Research and Innovation Future Leader
728   Fellowship (MR/V022792/1). SD acknowledges the Simons Collaboration on Computational Biogeochemical
729   Modelling of Marine Ecosystem (CBIOMES) (549931). BJ was supported by NASA (80NSSC21K0563,
730   Lagrangian analyses of ocean color and 80LARC21DA002 – GLIMR). ZK and MBK were supported in part by
731   the Croatian Science Foundation under the project number IP-2022-10-8859. FM thanks NERC for its support
732   (NE/X001261/1), RS is funded by the UKRI-NERC TerraFIRMA (NE/W004895/1) project, OU was supported
733   by a Royal Society Wolfson Visiting Fellowship (grant RSWVF\R3\223016), JT acknowledges the European
734   Union's Horizon 2020 (grant no. 817578), the European Union under grant agreement no. 101083922 (OceanICU)
735   and UK Research and Innovation (UKRI) under the UK government's Horizon Europe funding guarantee (grant
736   numbers 10054454, 10063673, 10064020, 10059241, 10079684, 10059012, 10048179).

737
738   **References**

739   Amirian, M. M., Finkel, Z. V., Devred, E., Irwin, A. J. (accepted). Parametrization of Photoinhibition for
740   Phytoplankton. Communications Earth and Environment.

742   Anderson, S.I., A.D. Barton, S. Clayton, S. Dutkiewicz, and T. Rynearson, 2021.Marine phytoplankton functional
743   types exhibit diverse responses to thermal change. Nature Communications, doi:10.1038/s41467-021-26651

745   Antoine D, Andre J-M, Morel A (1996). Oceanic primary production: 2. Estimation at global scale from satellite
746   (Coastal Zone Color Scanner) chlorophyll. Global Biogeochemical Cycles, 10:57-69.
747   https://doi.org/10.1029/95GB02832

749   Arteaga, L.A., Behrenfeld, M.J., Boss, E. and Westberry, T.K., 2022. Vertical structure in phytoplankton growth
750   and productivity inferred from biogeochemical-Argo floats and the carbon-based productivity model. *Global*
751   *Biogeochemical Cycles*, *36*(8), p.e2022GB007389.

753   Behrenfeld, M.J. and Falkowski, P.G. (1997) Photosynthetic Rates Derived from Satellite-based Chlorophyll
754   Concentration. Limnology and Oceanography, 42, 1-20. https://doi.org/10.4319/lo.1997.42.1.0001

756   Behrenfeld MJ, Boss E, Siegel D, and Shea DM (2005) Carbon-based ocean productivity and phytoplankton
757   physiology from space. Global Biogeochemical Cycles 19. https://doi.org/10.1029/2004GB002299.

759   Bergas-Masso, E., Hamilton, D.S., Myriokefalitakis, S., Rathod, S., Gonçalves Ageitos, M. and Pérez García-
760   Pando, C., 2025. Future climate-driven fires may boost ocean productivity in the iron-limited North
761   Atlantic. *Nature Climate Change*, pp.1-9.

763   Blackford, J. C., Allen, J. I., and Gilbert, F. J.: Ecosystem dynamics at six contrasting sites: a generic modelling
764   study, J. Marine Syst., 52, 191–215, 2004

766   Bopp, L., Resplandy, L., Orr, J. C., Doney, S. C., Dunne, J. P., Gehlen, M., Halloran, P., Heinze, C., Ilyina, T.,
767   Séférian, R., Tjiputra, J., and Vichi, M.: Multiple stressors of ocean ecosystems in the 21st century: projections
768   with CMIP5 models, Biogeosciences, 10, 6225–6245, https://doi.org/10.5194/bg-10-6225-2013, 2013.

770   Bopp, L., Aumont, O., Kwiatkowski, L., Clerc, C., Dupont, L., Ethé, C., Gorgues, T., Séférian, R., and Tagliabue,
771   A.: Diazotrophy as a key driver of the response of marine net primary productivity to climate change,
772   Biogeosciences, 19, 4267–4285, https://doi.org/10.5194/bg-19-4267-2022, 2022

774   Bouman, H.A., Platt, T., Doblin, M., Figueiras, M.G., Gudmundsson, K., Gudfinnsson, H.G., Huang, B.,
775   Hickman, A., Hiscock, M., Jackson, T., Lutz, V.A., Mélin, F., Rey, F., Pepin, P., Segura, V., Tilstone, G.H., van
776   Dongen-Vogels, V., Sathyendranath, S. (2018) Photosynthesis–irradiance parameters of marine phytoplankton:
777   synthesis of a global data set. Earth Syst. Sci. Data, 10: 251–266. https://doi.org/10.5194/essd-10-251-2018
778

779 RJW Brewin, GH Tilstone, T Jackson, T Cain, PI Miller (2017) Modelling size-fractionated primary production
780 in the Atlantic Ocean from remote sensing. Progress in Oceanography. 158: 130-149, ISSN 0079-6611,
781 https://doi.org/10.1016/j.pocean.2017.02.002.

783 Brewin, R.J., Sathyendranath, S., Kulk, G., Rio, M.H., Concha, J.A., Bell, T.G., Bracher, A., Fichot, C., Frölicher,
784 T.L., Galí, M. and Hansell, D.A., 2023. Ocean carbon from space: Current status and priorities for the next
785 decade. *Earth-science reviews*, *240*, p.104386.

787 Butenschön, M., Clark, J., Aldridge, J.N., Allen, J.I., Artioli, Y., Blackford, J., Bruggeman, J., Cazenave, P.,
788 Ciavatta, S., Kay, S., Lessin, G. *et al.*, 2016. ERSEM 15.06: a generic model for marine biogeochemistry and the
789 ecosystem dynamics of the lower trophic levels. *Geoscientific Model Development*, *9*(4), pp.1293-1339.

791 Carr, M.E., Friedrichs, M.A., Schmeltz, M., Aita, M.N., Antoine, D., Arrigo, K.R., Asanuma, I., Aumont, O.,
792 Barber, R., Behrenfeld, M. and Bidigare, R., 2006. A comparison of global estimates of marine primary production
793 from ocean color. *Deep Sea Research Part II: Topical Studies in Oceanography*, *53*(5-7), pp.741-770.

795 Chai, F., Johnson, K.S., Claustre, H., Xing, X., Wang, Y., Boss, E., Riser, S., Fennel, K., Schofield, O. and Sutton,
796 A., 2020. Monitoring ocean biogeochemistry with autonomous platforms. *Nature Reviews Earth & Environment*,
797 *Environment*, *1*(6), pp.315-326.

799 Ciavatta, S., Lazzari, P., Álvarez, E., Bertino, L., Bolding, K., Bruggeman, J., Capet, A., Cossarini, G., Daryabor,
800 F., Nerger, L., Popov, M. *et al.*, 2025. Control of simulated ocean ecosystem indicators by biogeochemical
801 observations. *Progress in Oceanography*, *231*, p.103384.

803 Claustre, H, and Johnson, KS, and Takeshita, Y (2020) Observing the Global Ocean with Biogeochemical-Argo.
804 Annual Review of Marine Science,12: 23-48. https://doi.org/10.1146/annurev-marine-010419-010956

806 Daewel, U. and Schrum, C., 2013. Simulating long-term dynamics of the coupled North Sea and Baltic Sea
807 ecosystem with ECOSMO II: Model description and validation. *Journal of Marine Systems*, *119*, pp.30-49.

809 Dai, R., Wen, Z., Hong, H., Browning, T.J., Hu, X., Chen, Z., Liu, X., Dai, M., Morel, F.M. and Shi, D., 2025.
810 Eukaryotic phytoplankton drive a decrease in primary production in response to elevated CO2 in the tropical and
811 subtropical oceans. *Proceedings of the National Academy of Sciences*, *122*(11), p.e2423680122.

813 Doléac, S., Lévy, M., El Hourany, R., and Bopp, L.: Toward more robust net primary production projections in
814 the North Atlantic Ocean, Biogeosciences, 22, 841–862, https://doi.org/10.5194/bg-22-841-2025, 2025.

816 Doney, S., Bopp, L., Long, M (2014) Historical and Future Trends in Ocean Climate and Biogeochemistry.
817 Oceanography. 27 (1), pp.108-119. ff10.5670/oceanog.2014.14ff. ffhal-03211060f

819 Doron M, Brasseur P, Brankart JM, Losa SN, Melet A. Stochastic estimation of biogeochemical parameters from
820 Globcolour ocean colour satellite data in a North Atlantic 3D ocean coupled physical–biogeochemical model.
821 Journal of Marine Systems. 2013 May 1;117:81-95.

823 Droop, M. R.: The nutrient status of alga cells in continous culture, J. Mar. Biol. Assoc. UK, 54, 825–855,
824 doi:10.1016/0924-7963(94)00031-6, 1974

826 Dutkiewicz, S., J.R. Scott, and M.J. Follows, 2013, Winners and Losers: Ecological and Biogeochemical Changes
827 in a Warming Ocean. Global Biogeochemical Cycles, 27, 463-477, doi: 10.1002/gbc.20042

829 Dutkiewicz, S., Hickman, A.E., Jahn, O., Gregg, W.W., Mouw, C.B. and Follows, M.J., 2015. Capturing optically
830 important constituents and properties in a marine biogeochemical and ecosystem model. *Biogeosciences*, *12*(14),
831 pp.4447-4481.

833 Dutkiewicz, S., Cermeno, P., Jahn, O., Follows, M.J., Hickman, A.E., Taniguchi, D.A. and Ward, B.A., 2020.
834 Dimensions of marine phytoplankton diversity. *Biogeosciences*, *17*(3), pp.609-634.

836 Fasham, MJR, Ducklow, HW, McKelvie, SM (1990) A nitrogen-based model of plankton dynamics in the oceanic
837 mixed layer. Journal of Marine Research, 48: 591-639.

839 Fennel, K., Gehlen, M., Brasseur, P., Brown, C.W., Ciavatta, S., Cossarini, G., Crise, A., Edwards, C.A., Ford,
840 D., Friedrichs, M.A. and Gregoire, M., 2019. Advancing marine biogeochemical and ecosystem reanalyses and
841 forecasts as tools for monitoring and managing ecosystem health. *Frontiers in Marine Science*, *6*, p.89.

843 Fennel, K., Mattern, J.P., Doney, S.C., Bopp, L., Moore, A.M., Wang, B. and Yu, L., 2022. Ocean biogeochemical
844 modelling. *Nature Reviews Methods Primers*, *2*(1), p.76.

846 Field, CB, Behrenfeld, MJ, Randerson, JT, Falkowski, P (1998) Primary Production of the Biosphere: Integrating
847 terrestrial and oceanic Components. Science 281, 237-240. DOI: 10.1126/science.281.5374.237

849 Flynn, K.J. and Mitra, A., 2023. Feeding in mixoplankton enhances phototrophy increasing bloom-induced pH
850 changes with ocean acidification. *Journal of Plankton Research*, *45*(4), pp.636-651.

852 Franks, P.J.S., 2002. NPZ models of plankton dynamics: their construction, coupling to physics, and application.
853 J. Oceanogr. 58, 379–387. DOI: 10.1023/a:1015874028196.

855 Friedlingstein, P., O'Sullivan, M., Jones, M. W., Andrew, R. M., Bakker, D. C. E., Hauck, J., Landschützer, P.,
856 Le Quéré, C., Luijkx, I. T., Peters, G. P., Peters, W., Pongratz, J., Schwingshackl, C., Sitch, S., Canadell, J. G.,
857 Ciais, P., Jackson, R. B., Alin, S. R., Anthoni, P., Barbero, L., Bates, N. R., Becker, M., Bellouin, N., Decharme,
858 B., Bopp, L., Brasika, I. B. M., Cadule, P., Chamberlain, M. A., Chandra, N., Chau, T.-T.-T., Chevallier, F., Chini,

859   L. P., Cronin, M., Dou, X., Enyo, K., Evans, W., Falk, S., Feely, R. A., Feng, L., Ford, D. J., Gasser, T., Ghattas,

860   J., Gkritzalis, T., Grassi, G., Gregor, L., Gruber, N., Gürses, Ö., Harris, I., Hefner, M., Heinke, J., Houghton, R.

861   A., Hurtt, G. C., Iida, Y., Ilyina, T., Jacobson, A. R., Jain, A., Jarníková, T., Jersild, A., Jiang, F., Jin, Z., Joos, F.,

862   Kato, E., Keeling, R. F., Kennedy, D., Klein Goldewijk, K., Knauer, J., Korsbakken, J. I., Körtzinger, A., Lan,

863   X., Lefèvre, N., Li, H., Liu, J., Liu, Z., Ma, L., Marland, G., Mayot, N., McGuire, P. C., McKinley, G. A., Meyer,

864   G., Morgan, E. J., Munro, D. R., Nakaoka, S.-I., Niwa, Y., O'Brien, K. M., Olsen, A., Omar, A. M., Ono, T.,

865   Paulsen, M., Pierrot, D., Pocock, K., Poulter, B., Powis, C. M., Rehder, G., Resplandy, L., Robertson, E.,

866   Rödenbeck, C., Rosan, T. M., Schwinger, J., Séférian, R., Smallman, T. L., Smith, S. M., Sospedra-Alfonso, R.,

867   Sun, Q., Sutton, A. J., Sweeney, C., Takao, S., Tans, P. P., Tian, H., Tilbrook, B., Tsujino, H., Tubiello, F., van

868   der Werf, G. R., van Ooijen, E., Wanninkhof, R., Watanabe, M., Wimart-Rousseau, C., Yang, D., Yang, X., Yuan,

869   W., Yue, X., Zaehle, S., Zeng, J., and Zheng, B.: Global Carbon Budget 2023, Earth Syst. Sci. Data, 15, 5301–

870   5369, https://doi.org/10.5194/essd-15-5301-2023, 2023.

871

872   Garcia, H.E., Weathers, K.W., Paver, C.R., Smolyar, I., Boyer, T.P., Locarnini, M.M., Zweng, M.M., Mishonov,

873   A.V., Baranova, O.K. and Seidov, D., 2019. World ocean atlas 2018. Vol. 4: Dissolved inorganic nutrients

874   (phosphate, nitrate and nitrate+ nitrite, silicate).

875

876   Gharamti ME, Samuelsen A, Bertino L, Simon E, Korosov A, Daewel U. Online tuning of ocean biogeochemical

877   model parameters using ensemble estimation techniques: Application to a one-dimensional model in the North

878   Atlantic. Journal of Marine Systems. 2017 Apr 1;168:1-6.

879

880   Gharamti ME, Tjiputra J, Bethke I, Samuelsen A, Skjelvan I, Bentsen M, Bertino L. Ensemble data assimilation

881   for ocean biogeochemical state and parameter estimation at different sites. Ocean Modelling. 2017 Apr 1;112:65-

882   89.

883

884   Gregg, W.W. and Rousseaux, C.S., 2016. Directional and spectral irradiance in ocean models: Effects on

885   simulated global phytoplankton, nutrients, and primary production. *Frontiers in Marine Science*, *3*, p.240.

886

887   Grégoire, M. and Soetaert, K., 2010. Carbon, nitrogen, oxygen and sulfide budgets in the Black Sea: A

888   biogeochemical model of the whole water column coupling the oxic and anoxic parts. *Ecological Modelling*,

889   *221*(19), pp.2287-2301.

890

891   Eppley, R., 1971. Temperature and phytoplankton growth in the sea. *Fishery bulletin*, *70*(4), p.1063

892

893   Friedlingstein, P., O'sullivan, M., Jones, M.W., Andrew, R.M., Hauck, J., Landschützer, P., Le Quéré, C., Li, H.,

894   Luijkx, I.T., Olsen, A. and Peters, G.P., 2024. Global carbon budget 2024. *Earth System Science Data*

895   *Discussions*, *2024*, pp.1-133.

896

897   Friedrichs, M.A., Dusenberry, J.A., Anderson, L.A., Armstrong, R.A., Chai, F., Christian, J.R., Doney, S.C.,

898   Dunne, J., Fujii, M., Hood, R. and McGillicuddy Jr, D.J., 2007. Assessment of skill and portability in regional

899   marine biogeochemical models: Role of multiple planktonic groups. *Journal of Geophysical Research: Oceans*,

900   *112*(C8).

901

902   Friedrichs, M.A.M., Carr, M.-E., Barber, R.T., Scardi, M., Antoine, D., Armstrong, R. A.,*et al.* (2009) Assessing

903   the uncertainties of model estimates of primary productivity in the tropical Pacific Ocean. J. Mar. Syst. 76, 113-

904   133. doi:10.1016/j.jmarsys.2008.05.010

905

906   Frölicher, T. L., K. B. Rodgers, C. A. Stock, and W. W. L. Cheung (2016), Sources of uncertainties in 21st century

907   projections of potential ocean ecosystem stressors, Global Biogeochem. Cycles, 30, 1224–1243,

908   doi:10.1002/2015GB005338.

909

910   Galli, G., Wakelin, S., Harle, J., Holt, J., Artioli, Y., 2024. Multi-model comparison of trends and controls of near-

911   bed oxygen concentration on the northwest European continental shelf under climate change. Biogeosciences 21,

912   2143–2158. https://doi.org/10.5194/bg-21-2143-2024

913

914   Gastineau, G., & Soden, B. J. (2009). Model projected changes of extreme wind events in response to global

915   warming. *Geophysical Research Letters*, *36*(10). https://doi.org/10.1029/2009GL037500

916

917   Geider, RJ, Macintyre, HL, and Kana, TM (1997) Dynamic model of phytoplankton growth and acclimation:

918   responses of the balanced growth rate and the chlorophyll a: carbon ratio to light, nutrient imitation and

919   temperature," Mar. Ecol. Prog. Ser. 148, 187–200.

920

921   Geider RJ, MacIntyre HL, Kana TM. (1998) A dynamic regulatory model of phytoplankton acclimation to light,

922   nutrients, and temperatures. Limnol. Oceanogr., 43(4), 679-694.

923

924   Gentile, E. S., Zhao, M., & Hodges, K. (2023). Poleward intensification of midlatitude extreme winds under

925   warmer climate. *Npj Climate and Atmospheric Science*, *6*(1), 1–10. https://doi.org/10.1038/s41612-023-00540-x

926

927   Gentleman, W., 2002. A chronology of plankton dynamics in silico: how computer models have been used to

928   study marine ecosystems. Hydrobiologia 480, 69–85. DOI: 10.1023/A:1021289119442.

929

930   Gregg W.W and Rousseaux C.S. 2019. Global ocean primary production trends in the modern ocean color satellite

931   record (1998–2015). Environ. Res. Lett. 14 124011

932

933   Grégoire, M., Raick, C. and Soetaert, K., 2008. Numerical modeling of the central Black Sea ecosystem

934   functioning during the eutrophication phase. *Progress in Oceanography*, *76*(3), pp.286-333.

935

936   Grégoire, M. and Soetaert, K., 2010. Carbon, nitrogen, oxygen and sulfide budgets in the Black Sea: A

937   biogeochemical model of the whole water column coupling the oxic and anoxic parts. *Ecological Modelling*,

938   *221*(19), pp.2287-2301.

939

940 Gulev, S.K., P.W. Thorne, J. Ahn, F.J. Dentener, C.M. Domingues, S. Gerland, D. Gong, D.S. Kaufman, H.C.
941 Nnamchi, J. Quaas, J.A. Rivera, S. Sathyendranath, S.L. Smith, B. Trewin, K. von Schuckmann, and R.S. Vose,
942 2021: Changing State of the Climate System. In Climate Change 2021: The Physical Science Basis. Contribution
943 of Working Group I to the Sixth Assessment Report of the Intergovernmental Panel on Climate Change [Masson-
944 Delmotte, V., P. Zhai, A. Pirani, S.L. Connors, C. Péan, S. Berger, N. Caud, Y. Chen, L. Goldfarb, M.I. Gomis,
945 M. Huang, K. Leitzell, E. Lonnoy, J.B.R. Matthews, T.K. Maycock, T. Waterfield, O. Yelekçi, R. Yu, and B.
946 Zhou (eds.)]. Cambridge University Press, Cambridge, United Kingdom and New York, NY, USA, pp. 287–422,
947 doi: 10.1017/9781009157896.004.

948

949 Halsey, K.H., Milligan, A.J. and Behrenfeld, M.J., 2011. Linking time-dependent carbon-fixation efficiencies in
950 Dunaliella Tertiolecta (Chlorophyceae) to underlying metabolic pathways 1. *Journal of Phycology*, *47*(1), pp.66-
951 76.

952

953 Henson, S., Baker, C.A., Halloran, P., McQuatters-Gollop, A., Painter, S., Planchat, A. and Tagliabue, A., 2024.
954 Knowledge gaps in quantifying the climate change response of biological storage of carbon in the ocean. *Earth's
955 Future*, *12*(6), p.e2023EF004375.

956

957 Hewitt, C. D., and Coauthors, 2021: Recommendations for Future Research Priorities for Climate Modeling and
958 Climate Services. Bull. Amer. Meteor. Soc., 102, E578–E588, https://doi.org/10.1175/BAMS-D-20-0103.1.

959

960 IOCCG (2020). Synergy between Ocean Colour and Biogeochemical/Ecosystem Models. Dutkiewicz, S. (ed.),
961 IOCCG Report Series, No. 19, International Ocean Colour Coordinating Group, Dartmouth, Canada.
962 http://dx.doi.org/10.25607/OBP-711

963

964 IOCCG Protocol Series (2022). Aquatic Primary Productivity Field Protocols for Satellite Validation and Model
965 Synthesis. Balch, W.M., Carranza, M., Cetinić, I., Chaves, J.E., Duhamel, S., Fassbender, A., Fernandez-Carrera,
966 A., Ferrón, S., García-Martín, E., Goes, J., Gomes, H., Gundersen, K., Halsey, K., Hirawake, T., Isada, T., Juranek,
967 L., Kulk, G., Langdon, C., Letelier, R., López-Sandoval, D., Mannino, A., Marra, J.F., Neale, P., Nicholson, D.,
968 Silsbe, G., Stanley, R.H., Vandermeulen, R.A. IOCCG Ocean Optics and Biogeochemistry Protocols for Satellite
969 Ocean Colour Sensor Validation, Volume 7.0, edited by R.A. Vandermeulen, J. E. Chaves, IOCCG, Dartmouth,
970 NS, Canada. doi:http://dx.doi.org/10.25607/OBP-1835

971

972 IPCC (2019): IPCC Special Report on the Ocean and Cryosphere in a Changing Climate [H.-O. Pörtner, D.C.
973 Roberts, V. Masson-Delmotte, P. Zhai, M. Tignor, E. Poloczanska, K. Mintenbeck, A. Alegría, M. Nicolai, A.
974 Okem, J. Petzold, B. Rama, N.M. Weyer (eds.)].

975

976 IPCC, 2021: Climate Change 2021 - the Physical Science Basis, Contribution of Working Group I to the Sixth
977 Assessment Report of the Intergovernmental Panel on Climate Change [Masson-Delmotte, V., P. Zhai, A. Pirani,
978 S.L. Connors, C. Péan, S. Berger, N. Caud, Y. Chen, L. Goldfarb, M.I. Gomis, M. Huang, K. Leitzell, E. Lonnoy,

979   J.B.R. Matthews, T.K. Maycock, T. Waterfield, O. Yelekçi, R. Yu, and B. Zhou (eds.)]. Cambridge University
980   Press, In Press, Published: 9 August 2021.

981

982   Jackson, T, Sathyendranath, S, and T. Platt, T (2017) An exact solution for modeling photoacclimation of the
983   carbon-to-chlorophyll ratio in phytoplankton, Front. Mar. Sci. 4, 283

984

985   Jassby, A.D. and Platt, T., 1976. Mathematical formulation of the relationship between photosynthesis and light
986   for phytoplankton. *Limnology and oceanography*, *21*(4), pp.540-547.

987

988   Jin, P., Hutchins, D.A. and Gao, K., 2020. The impacts of ocean acidification on marine food quality and its
989   potential food chain consequences. *Frontiers in Marine Science*, *7*, p.543979.

990

991   Jones, C. G., Adloff, F., Booth, B., Cox, P., Eyring, V., Friedlingstein, P., Frieler, K., Hewitt, H., Jeffery, H.,
992   Joussaume, S., Koenigk, T., Lawrence, B. N., O'Rourke, E., Roberts, M., Sanderson, B., Séférian, R., Somot, S.,
993   Vidale, P.-L., van Vuuren, D., Acosta, M., Bentsen, M., Bernardello, R., Betts, R., Blockley, E., Boé, J.,
994   Bracegirdle, T., Braconnot, P., Brovkin, V., Buontempo, C., Doblas-Reyes, F. J., Donat, M. G., Epicoco, I.,
995   Falloon, P., Fiore, S., Froelicher, T., Fuckar, N., Gidden, M., Goessling, H., Graversen, R. G., Gualdi, S.,
996   Gutiérrez, J. M., Ilyina, T., Jacob, D., Jones, C., Juckes, M., Kendon, E., Kjellström, E., Knutti, R., Lowe, J. A.,
997   Mizielinski, M., Nassisi, P., Obersteiner, M., Regnier, P., Roehrig, R., Salas y Melia, D., Schleussner, C.-F.,
998   Schulz, M., Scoccimarro, E., Terray, L., Thiemann, H., Wood, R., Yang, S., and Zaehle, S.: Bringing it all
999   together: Science and modelling priorities to support international climate policy, EGUsphere [preprint],
1000   https://doi.org/10.5194/egusphere-2024-453, 2024.

1001

1002   Kiefer, D.A. and Mitchell, B.G., 1983. A simple, steady state description of phytoplankton growth based on
1003   absorption cross section and quantum efficiency 1. *Limnology and Oceanography*, *28*(4), pp.770-776.

1004

1005   Kim, H.H., Laufkötter, C., Lovato, T., Doney, S.C. and Ducklow, H.W., 2023. Projected 21st-century changes in
1006   marine heterotrophic bacteria under climate change. *Frontiers in microbiology*, *14*, p.1049579.

1007

1008   Kishi, M.J., Kashiwai, M., Ware, D.M., Megrey, B.A., Eslinger, D.L., Werner, F.E., Noguchi-Aita, M., Azumaya,
1009   T., Fujii, M., Hashimoto, S. and Huang, D., 2007. NEMURO—a lower trophic level model for the North Pacific
1010   marine ecosystem. *Ecological Modelling*, *202*(1-2), pp.12-25.

1011

1012   Kovač, Ž., Platt, T., Sathyendranath, S., Morović, M., Jackson, T. (2016a). Recovery of photosynthesis parameters
1013   from in situ profiles of phytoplankton production. ICES Journal of Marine Science, 73 (2), 275–285. DOI:
1014   10.1093/icesjms/fsv204.

1015

1016   Kovač, Ž., Platt, T., Sathyendranath, S., Morović, M. (2016b). Analytical solution for the vertical profile of daily
1017   production in the ocean. Journal of Geophysical Research: Oceans, 121. DOI: 10.1002/2015JC011293.

1018

1019 Kovač, Ž., Platt, T., S., S., Antunović, S. (2017). Models for estimating photosynthesis parameters from in situ
1020 production profiles. Progress in Oceanography, 159, 255-266. doi:10.1016/j.pocean.2017.10.013.

1022 Kovač, Ž., Platt, T., Sathyendranath, S., Lomas, M. W. (2018). Extraction of photosynthesis parameters from time
1023 series measurements of in situ production: Bermuda atlantic time-series study. Remote Sensing, 10, 915. DOI:
1024 10.3390/rs10060915.

1026 Kovárová-Kovar, K. and Egli, T., 1998. Growth kinetics of suspended microbial cells: from single-substrate-
1027 controlled growth to mixed-substrate kinetics. *Microbiology and molecular biology reviews*, *62*(3), pp.646-666.

1029 Krinos, A.I., Shapiro, S.K., Li, W., Haley, S.T., Dyhrman, S.T., Dutkiewicz, S., Follows, M.J. and Alexander, H.
1030 (2025), Intraspecific Diversity in Thermal Performance Determines Phytoplankton Ecological Niche. Ecology
1031 Letters, 28: e70055. https://doi.org/10.1111/ele.70055

1033 Kulk, G, Platt, T, Dingle, J, Jackson, T, Jönsson, BF, Bouman, HA, Babin, M, Brewin, RJW, Doblin, M, Estrada,
1034 M, Figueiras, FG, Furuya, K, González-Benítez, N, Gudfinnsson, HG, Gudmundsson, K, Huang, B, Isada, T,
1035 Kovač, Ž, Lutz, VA, Marañón, E, Raman, M, Richardson, K, Rozema, PD, Poll, WH, Segura, V, Tilstone, GH,
1036 Uitz, J, Dongen-Vogels, V, Yoshikawa, T, Sathyendranath, S (2020) Primary Production, an Index of Climate
1037 Change in the Ocean: Satellite-Based Estimates over Two Decades. Remote Sensing, 12, 826.
1038 https://doi.org/10.3390/rs12050826

1040 Kulk, G.; Platt, T.; Dingle, J.; Jackson, T.; Jönsson, B.F.; Bouman, H.A.; Babin, M.; Brewin, R.J.W.; Doblin, M.;
1041 Estrada, M.; *et al*. Correction: Kulk *et al*. Primary Production, an Index of Climate Change in the Ocean: Satellite-
1042 Based Estimates over Two Decades. Remote Sens. 2020, 12, 826. Remote Sens. 2021, 13, 3462.
1043 https://doi.org/10.3390/rs13173462

1045 Kyewalyanga, M., Platt, T., & Sathyendranath, S. (1992). Ocean primary production calculated by spectral and
1046 broadband models. Marine Ecology Progress Series, 85, 171–185. DOI: 10.3354/meps085171.

1048 Kyewalyanga, MN, Platt, T, Sathyendranath, S (1997) Estimation of the photosynthetic action spectrum:
1049 implications for primary production models. *Mar. Ecol. Prog. Ser.* 146: 207-223.

1051 Kwiatkowski, L., Bopp, L., Aumont, O., Ciais, P., Cox, P.M., Laufkötter, C., Li, Y. and Séférian, R., 2017.
1052 Emergent constraints on projections of declining primary production in the tropical oceans. *Nature Climate
1053 Change*, *7*(5), pp.355-358.

1055 Kwiatkowski, L., Torres, O., Bopp, L., Aumont, O., Chamberlain, M., Christian, J.R., Dunne, J.P., Gehlen, M.,
1056 Ilyina, T., John, J.G., Lenton, A., Li, H., Lovenduski, N.S., Orr, J.C., Palmieri, J., Santana-Falcón, Y., Schwinger,
1057 J., Séférian, R., Stock, C.A., Tagliabue, A., Takano, Y., Tjiputra, J., Toyama, K., Tsujino, H., Watanabe, M.,
1058 Yamamoto, A., Yool, A., Ziehn, T., 2020. Twenty-first century ocean warming, acidification, deoxygenation, and

1059   upper-ocean nutrient and primary production decline from CMIP6 model projections. Biogeosciences 17, 3439–
1060   3470. https://doi.org/10.5194/bg-17-3439-2020

1061

1062   Laufkötter, C., Vogt, M., Gruber, N., Aita-Noguchi, M., Aumont, O., Bopp, L., Buitenhuis, E., Doney, S. C.,
1063   Dunne, J., Hashioka, T., Hauck, J., Hirata, T., John, J., Le Quéré, C., Lima, I. D., Nakano, H., Seferian, R.,
1064   Totterdell, I., Vichi, M., and Völker, C. (2015) Drivers and uncertainties of future global marine primary
1065   production in marine ecosystem models, Biogeosciences, 12, 6955–6984, https://doi.org/10.5194/bg-12-6955-
1066   2015

1067

1068   Lee, Z. Veronica P. Lance, VP, Shang, S, Vaillancourt,R, Freeman,S, Lubac, B, Hargreaves, BR, Del Castillo, C,
1069   Richard Miller, R, Twardowski, M, Wei, G (2011) An assessment of optical properties and primary production
1070   derived from remote sensing in the Southern Ocean (SO GasEx). J. Geophys. Res. 116, C00F03 (2011).
1071   doi:10.1029/2010JC006747.

1072

1073   Lee Z, Marra J, Perry MJ, Kahru M (2015). Estimating oceanic primary productivity from ocean color remote
1074   sensing: A strategic assessment, Journal of Marine Systems. http://dx.doi.org/10.1016/j.jmarsys.2014.11.015Lee,
1075   S. and Yoo, S. (2016) 'Interannual variability of the phytoplankton community by the changes in vertical mixing
1076   and atmospheric deposition in the Ulleung Basin, East Sea: A modelling study', Ecological Modelling, 322, pp.
1077   31–47. Available at: https://doi.org/10.1016/j.ecolmodel.2015.11.012.

1078

1079   Lee, Y. J., P. A. Matrai, M. A. M. Friedrichs, V. S. Saba, D. Antoine, M. Ardyna, I. Asanuma, M. Babin, S.
1080   Belanger, M. Benoıt-Gagne, E. Devred, M. Fernandez-Mendez, B. Gentili, T. Hirawake, S.-H. Kang, T. Kameda,
1081   C. Katlein, S.H. Lee, Z. Lee, F. Melin, M. Scardi, T.J. Smyth, S. Tang, K.R. Turpie, K.J. Waters, and T.K.
1082   Westberry (2015). An assessment of ocean color model estimates of primary productivity in the Arctic Ocean. J.
1083   Geophys. Res. Oceans, FAMOS SI, 120:6508–6541, DOI 10.1002/2015JC011018.

1084

1085   Liu, H., Li, D., Chen, Q., Feng, J., Qi, J., & Yin, B. (2024). The multiscale variability of global extreme wind and
1086   wave events and their relationships with climate modes. *Ocean Engineering*, *307*, 118239.
1087   https://doi.org/10.1016/j.oceaneng.2024.118239

1088

1089   Longhurst, A, Sathyendranath, S, Platt, T, Caverhill, C (1995) An estimate of global primary production in the
1090   ocean from satellite radiometer data. J. Plankton Res. 17: 1245-1271.

1091

1092   Longhurst, A.R. Ecological Geography of the Sea, 2nd ed.; Elsevier Academic Press: Cambridge, MA, USA,
1093   2007; p. 542.

1094

1095   Löptien, U. and Dietze, H., 2019. Reciprocal bias compensation and ensuing uncertainties in model-based climate
1096   projections: pelagic biogeochemistry versus ocean mixing. *Biogeosciences*, *16*(9), pp.1865-1881.

1097

1098   Lurin, B., Rasool,S.I., Cramer.W. and Moore.B. (1994) Global terrestrial net primary production. Glob. Change
1099   NewsL (IGBP), 19, 6-8.

1101   Luypaert, T., Hagan, J.G., McCarthy, M.L. and Poti, M., 2020. Status of marine biodiversity in the
1102   Anthropocene. *YOUMARES*, *9*, pp.57-82.

1104   Maishal, S., 2024. Decadal changes in global Oceanic Primary Productivity and its drivers. *Ocean-Land-*
1105   *Atmosphere Research*, *3*, p.0066.

1107   Marshak, A.R., Link, J.S. Primary production ultimately limits fisheries economic performance. Sci Rep 11,
1108   12154 (2021). https://doi.org/10.1038/s41598-021-91599-0

1110   Michaelis L, Menten ML. Die kinetik der invertinwirkung. Biochem. z. 1913 Feb;49(333-369):352.

1112   Mitra, A., Caron, D.A., Faure, E., Flynn, K.J., Leles, S.G., Hansen, P.J., McManus, G.B., Not, F., do Rosario
1113   Gomes, H., Santoferrara, L.F. and Stoecker, D.K., 2023. The Mixoplankton Database (MDB): Diversity of photo-
1114   phago-trophic plankton in form, function, and distribution across the global ocean. *Journal of Eukaryotic*
1115   *Microbiology*, *70*(4), p.e12972.

1117   Myksvoll, M.S., Sandø, A.B., Tjiputra, J., Samuelsen, A., Yumruktepe, V.Ç., Li, C., Mousing, E.A., Bettencourt,
1118   J.P. and Ottersen, G., 2023. Key physical processes and their model representation for projecting climate impacts
1119   on subarctic Atlantic net primary production: A synthesis. *Progress in Oceanography*, *217*, p.103084.

1121   Norberg J., Biodiversity and ecosystem functioning: A complex adaptive systems approach, Limnology and
1122   Oceanography, 4, part 2, doi: 10.4319/lo.2004.49.4_part_2.1269. 2004.

1124   T. Parsons, M. Takahashi, B. Hargrave., Biological Oceanographic Processes (Third edition), Pergamon
1125   International Library of Science, Technology, Engin, Pergamon (1984)

1127   Pastres, R., Ciavatta, S. and Solidoro, C., 2003. The Extended Kalman Filter (EKF) as a tool for the assimilation
1128   of high frequency water quality data. Ecological modelling, 170(2-3), pp.227-235.

1130   Platt, T., Gallegos, C.L. and Harrison, W.G., 1980. Photoinhibition of photosynthesis in natural assemblages of
1131   marine phytoplankton.

1133   Platt, T., Sathyendranath, S (1988) Oceanic primary production: Estimation by remote sensing at local and
1134   regional scales. Science 241: 1613-1620.

1136   Platt, T., Sathyendranath, S, Ravindran, P (1990) Primary production by phytoplankton: analytic solutions for
1137   daily rates per unit area of water surface. Proc. R. Soc. Lond. Ser. B 241: 101-111.

1138

1139   Platt, T, Sathyendranath, S (1991) Biological production models as elements of coupled, atmosphere-ocean

1140   models for climate research. J. Geophys. Res. 96: 2585-2592.

1141

1142   Platt, T, Sathyendranath, S (1993) Estimators of primary production for interpretation of remotely sensed data on

1143   ocean color. J. Geophys. Res. 98: 14,561-14,576.

1144   Platt, T, Sathyendranath, S (1997) Modelling primary production IV (in Japanese). *Aquabiology* 19: 229-232.

1145

1146   Radtke, H., Lipka, M., Bunke, D., Morys, C., Woelfel, J., Cahill, B., Böttcher, M.E., Forster, S., Leipe, T., Rehder,

1147   G. and Neumann, T., 2019. Ecological ReGional Ocean Model with vertically resolved sediments (ERGOM SED

1148   1.0): coupling benthic and pelagic biogeochemistry of the south-western Baltic Sea. *Geoscientific Model*

1149   *Development*, *12*(1), pp.275-320.

1150

1151   Ratnarajah L, Abu-Alhaija R, Atkinson A, Batten S, Bax NJ, Bernard KS, Canonico G, Cornils A, Everett JD,

1152   Grigoratou M, Ishak NH. Monitoring and modelling marine zooplankton in a changing climate. Nature

1153   Communications. 2023 Feb 2;14(1):564.

1154

1155   Regaudie-de-Gioux, A., Lasternas, S., Agustí, S., Duarte, C.M. 2019. Comparing marine primary production

1156   estimates through different methods and development of conversion equations. *Frontiers in Marine Science*, 1.

1157   URL: https://www.frontiersin.org/journals/marine-science/articles/10.3389/fmars.2014.00019.

1158   DOI=10.3389/fmars.2014.00019

1159

1160   Rohr T, Richardson AJ, Lenton A, Chamberlain MA, Shadwick EH. Zooplankton grazing is the largest source of

1161   uncertainty for marine carbon cycling in CMIP6 models. Communications Earth & Environment. 2023 Jun

1162   14;4(1):212.

1163

1164   Roy S, Broomhead DS, Platt T, Sathyendranath S, Ciavatta S. Sequential variations of phytoplankton growth and

1165   mortality in an NPZ model: A remote-sensing-based assessment. Journal of Marine Systems. 2012 Apr

1166   1;92(1):16-29.

1167

1168   Ryan-Keogh, T.J., Tagliabue, A. & Thomalla, S.J. Global decline in net primary production underestimated by

1169   climate models. *Commun Earth Environ* **6**, 75 (2025). https://doi.org/10.1038/s43247-025-02051-4

1170

1171   Saba, V.S., Friedrichs, M.A.M., Carr, M.-E., Antoine, D., Armstrong, R.A., Asanuma, I., *et al.*(2010) Challenges

1172   of modeling depth-integrated marine primary productivity over multiple decades: a case study at BATS and HOT.

1173   Glob. Biogeochem. Cycle 24, GB3020.doi:10.1029/2009GB003655

1174

1175   Sathyendranath, S., & Platt, T. (1989a). Computation of aquatic primary production: Extended formalism to

1176   include the effect of angular and spectral distribution of light. Limnology and Oceanography, 34, 188–198. DOI:

1177   10.4319/lo.1989.34.1.0188.

1178

1179 Sathyendranath, S, Platt, T, Caverhill, CM, Warnock, RE, Lewis, MR (1989b) Remote sensing of oceanic primary

1180 production: Computations using a spectral model. *Deep-Sea Res. I* 36: 431-453.

1181

1182 Sathyendranath, S, Platt, T (2007) Spectral effects in bio-optical control on the ocean system. Oceanologia 49: 5-

1183 39.

1184

1185 Sathyendranath, S, Stuart, V, Nair, A, Oka, K., Nakane, T, Bouman, H, Forget, M-H, Maass, H, Platt, T (2009)

1186 Carbon-to-chlorophyll ratio and growth rate of phytoplankton in the sea. Mar. Ecol. Prog. Ser. 383: 73–84, doi:

1187 10.3354/meps07998

1188

1189 Sathyendranath, S., Brewin, R., Brockmann, C., Brotas, V., Calton, B., Chuprin, A., *et al*. (2019). An ocean-

1190 colour time series for use in climate studies: The experience of the Ocean-Colour Climate Change Initiative (OC-

1191 CCI). Sensors, 19(19), 4285. https://doi.org/10.3390/s19194285

1192

1193 Sathyendranath, S, Platt, T, Kovač, Ž, Dingle, J, Jackson, T, Brewin, R JW, Franks, P, Marañón, E, Kulk, G, and

1194 Bouman, HA (2020) Reconciling models of primary production and photoacclimation [Invited]. Applied Optics,

1195 59: C100-C114. https://doi.org/10.1364/AO.386252

1196

1197 Sauterey B., Le Gland G., Cermeño P., Aumont O., Lévy M., Vallina S.M., Phytoplankton adaptive resilience to

1198 climate change collapses in case of extreme events – A modeling study. Ecological Modelling, Volume 483, 2023,

1199 110437, ISSN 0304-3800, https://doi.org/10.1016/-j.ecolmodel.2023.110437

1200

1201 Séférian, R., Berthet, S., Yool, A., Palmiéri, J., Bopp, L., Tagliabue, A., Kwiatkowski, L., Aumont, O., Christian,

1202 J., Dunne, J., Gehlen, M., Ilyina, T., John, J.G., Li, H., Long, M.C., Luo, J.Y., Nakano, H., Romanou, A.,

1203 Schwinger, J., Stock, C., Santana-Falcón, Y., Takano, Y., Tjiputra, J., Tsujino, H., Watanabe, M., Wu, T., Wu,

1204 F., Yamamoto, A., 2020. Tracking Improvement in Simulated Marine Biogeochemistry Between CMIP5 and

1205 CMIP6. Curr Clim Change Rep 6, 95–119. https://doi.org/10.1007/s40641-020-00160-0

1206

1207 Schartau, M., Wallhead, P., Hemmings, J., Löptien, U., Kriest, I., Krishna, S., Ward, B. A., Slawig, T., and

1208 Oschlies, A.: Reviews and syntheses: parameter identification in marine planktonic ecosystem modelling,

1209 Biogeosciences, 14, 1647–1701, https://doi.org/10.5194/bg-14-1647-2017, 2017.

1210

1211 Schmidtko S., Stramma L., Visbeck M. (2017). Decline in global oceanic oxygen content during the past five

1212 decades. *Nature* 542, 335–339. doi: 10.1038/nature21399

1213

1214 Shigemitsu, M., Okunishi, T., Nishioka, J., Sumata, H., Hashioka, T., Aita, M.N., Smith, S.L., Yoshie, N., Okada,

1215 N. and Yamanaka, Y., 2012. Development of a one-dimensional ecosystem model including the iron cycle applied

1216 to the Oyashio region, western subarctic Pacific. *Journal of Geophysical Research: Oceans*, *117*(C6).

1217

1218   Silsbe, G.M., Behrenfeld, M.J., Halsey, K.H., Milligan, A.J. and Westberry, T.K., 2016. The CAFE model: A net
1219   production model for global ocean phytoplankton. *Global Biogeochemical Cycles*, *30*(12), pp.1756-1777.

1220

1221   Silsbe, G.M., Fox, J., Westberry, T.K. *et al.* Global declines in net primary production in the ocean color era. *Nat*
1222   *Commun* **16**, 5821 (2025). https://doi.org/10.1038/s41467-025-60906-y

1223

1224   Simon E, Samuelsen A, Bertino L, Mouysset S. Experiences in multiyear combined state–parameter estimation
1225   with an ecosystem model of the North Atlantic and Arctic Oceans using the Ensemble Kalman Filter. Journal of
1226   Marine Systems. 2015 Dec 1;152:1-7.

1227

1228   Singh, T., Counillon, F., Tjiputra, J. and Wang, Y., 2025. A novel ensemble-based parameter estimation for
1229   improving ocean biogeochemistry in an Earth system model. *Journal of Advances in Modeling Earth*
1230   *Systems*, *17*(2), p.e2024MS004237.

1231

1232   Skákala, J., Wakamatsu, T., Bertino, L., Teruzzi, A., Lazzari, P., Alvarez, E., Cossarini, G.,Spada, S., Nerger, L.,
1233   Vliegen, S., Brankart, J. M., and Brasseur, P.: SEAMLESS Target indicator quality in CMEMS MFCs (D6.1),
1234   https://doi.org/10.5281/zenodo.10522305, 2024.

1235

1236   Smith, S.L., Yamanaka, Y., Pahlow, M. and Oschlies, A., 2009. Optimal uptake kinetics: physiological
1237   acclimation explains the pattern of nitrate uptake by phytoplankton in the ocean. *Marine Ecology Progress Series*,
1238   *384*, pp.1-12.

1239

1240   Steele, J.H., 1962. Environmental control of photosynthesis in the sea. *Limnology and oceanography*, *7*(2),
1241   pp.137-150.

1242

1243   Steele, J.H, Henderson, E.W. (1992) The role of predation in plankton models. Journal of Plankton Research,
1244   14(1): 157-172.

1245

1246   Steinacher, M., Joos, F., Frölicher, T. L., Bopp, L., Cadule, P., Cocco, V., Doney, S. C., Gehlen, M., Lindsay, K.,
1247   Moore, J. K., Schneider, B., and Segschneider, J.: Projected 21st century decrease in marine productivity: a multi-
1248   model analysis, Biogeosciences, 7, 979–1005, https://doi.org/10.5194/bg-7-979-2010, 2010

1249

1250   Stock, C.A., Dunne, J.P., Fan, S., Ginoux, P., John, J., Krasting, J.P., Laufkötter, C., Paulot, F. and Zadeh, N.,
1251   2020. Ocean biogeochemistry in GFDL's Earth System Model 4.1 and its response to increasing atmospheric CO2.
1252   *Journal of Advances in Modeling Earth Systems*, *12*(10), p.e2019MS002043.

1253

1254   Stock, C.A., Dunne, J.P., Luo, J.Y., Ross, A.C., Van Oostende, N., Zadeh, N., Cordero, T.J., Liu, X. and Teng,
1255   Y.C., 2025. Photoacclimation and photoadaptation sensitivity in a global ocean ecosystem model. *Journal of*
1256   *Advances in Modeling Earth Systems*, *17*(6), p.e2024MS004701.

1257

Tagliabue A, Kwiatkowski L, Bopp L, Butenschön M, Cheung W, Lengaigne M and Vialard J (2021) Persistent Uncertainties in Ocean Net Primary Production Climate Change Projections at Regional Scales Raise Challenges for Assessing Impacts on Ecosystem Services. Front. Clim. 3:738224. doi: 10.3389/fclim.2021.738224

Tao, Zui & Wang, Yan & Ma, Sheng & Lv, Tingting & Zhou, Xiang. (2017). A Phytoplankton Class-Specific Marine Primary Productivity Model Using MODIS Data. IEEE Journal of Selected Topics in Applied Earth Observations and Remote Sensing. PP. 1-10. 10.1109/JSTARS.2017.2747770.

Tjiputra, J.F., Polzin, D. and Winguth, A.M., 2007. Assimilation of seasonal chlorophyll and nutrient data into an adjoint three-dimensional ocean carbon cycle model: Sensitivity analysis and ecosystem parameter optimization. *Global biogeochemical cycles*, *21*(1).

Tjiputra, J.F., Couespel, D. and Sanders, R., 2025. Marine ecosystem role in setting up preindustrial and future climate. *Nature Communications*, *16*(1), p.2206.

Thomas, M.K., Kremer, C.T. and Litchman, E. (2016), Phytoplankton temperature trait biogeography. Global Ecology and Biogeography, 25: 75-86. https://doi.org/10.1111/geb.12387

Uitz J, Claustre H, Gentili B, Stramski D. (2010). Phytoplankton class-specific primary production in the world's oceans: Seasonal and interannual variability from satellite observations. Global Biogeochemical Cycles 24. https://doi.org/10.1029/2009GB003680

Vichi, M., Pinardi, N. and Masina, S., 2007. A generalized model of pelagic biogeochemistry for the global ocean ecosystem. Part I: Theory. *Journal of Marine Systems*, *64*(1-4), pp.89-109.

Ward, B.A., Dutkiewicz, S., Jahn, O. and Follows, M.J., 2012. A size-structured food-web model for the global ocean. *Limnology and Oceanography*, *57*(6), pp.1877-1891.

Webb, W.L., Newton, M. and Starr, D., 1974. Carbon dioxide exchange of Alnus rubra: a mathematical model. *Oecologia*, *17*, pp.281-291

Westberry, T., Behrenfeld, M.J., Siegel, D.A. and Boss, E., 2008. Carbon-based primary productivity modeling with vertically resolved photoacclimation. *Global Biogeochemical Cycles*, *22*(2).

Wu, Z., S. Dutkiewicz., O. Jahn, D. Sher, A. White, and M.J. Follows, 2021. Modeling photosynthesis and exudation in the subtropical oceans. Global Biogeochemical Cycles, 35, doi:10.1029/2021GB006941

Xiao, Y. and Friedrichs, M.A., 2014. Using biogeochemical data assimilation to assess the relative skill of multiple ecosystem models in the Mid-Atlantic Bight: effects of increasing the complexity of the planktonic food web. *Biogeosciences*, *11*(11), pp.3015-3030.

1298

1299 Yool, A., Popova, E.E. and Anderson, T.R., 2013. MEDUSA-2.0: an intermediate complexity biogeochemical

1300 model of the marine carbon cycle for climate change and ocean acidification studies. *Geoscientific Model*

1301 *Development*, *6*(5), pp.1767-1811.

1302

1303 Young, I. R., & Ribal, A. (2019). Multiplatform evaluation of global trends in wind speed and wave height.

1304 *Science*, *364*(6440), 548–552. https://doi.org/10.1126/science.aav9527

1305

1306 Yumruktepe, V.Ç., Samuelsen, A. and Daewel, U., 2022. ECOSMO II (CHL): a marine biogeochemical model

1307 for the North Atlantic and the Arctic. *Geoscientific Model Development*, *15*(9), pp.3901-3921.

1308

1309 Zheng, Q., Viljoen, J.J., Sun, X., Kovač, Ž., Sathyendranath, S. and Brewin, R.J., 2025. Simulating vertical

1310 phytoplankton dynamics in a stratified ocean using a two-layered ecosystem model. *Biogeosciences*, *22*(13),

1311 pp.3253-3278.

1312 .